The jet power, radio loudness and black hole mass in radio loud AGNs

Yi Liu [1,2,3], Dong Rong Jiang[1,2], Min Feng Gu[1,2]

ABSTRACT

The jet formation is thought to be closely connected with the mass of central supermassive black hole in Active Galactic Nuclei. The radio luminosity commonly used in investigating this issue is merely an indirect measure of the energy transported through the jets from the central engine, and severely Doppler boosted in core-dominated radio quasars. In this work, we investigate the relationship between the jet power and black hole mass, by estimating the jet power using extrapolated extended 151 MHz flux density from the VLA 5 GHz extended radio emission, for a sample of 146 radio loud quasars complied from literature. After removing the effect of relativistic beaming in the radio and optical emission, we find a significant intrinsic correlation between the jet power and black hole mass. It strongly implies that the jet power, so as jet formation, is closely connected with the black hole mass. To eliminate the beaming effect in the conventional radio loudness, we define a new radio loudness as the ratio of the radio extended luminosity to the optical luminosity estimated from the broad line luminosity. In a tentatively combined sample of radio quiet with our radio loud quasars, the apparent gap around the conventional radio loudness R=10 is not prominent for the new-defined radio loudness. In this combined sample, we find a significant correlation between the black hole mass and new-defined radio loudness.

Subject headings: black hole physics – galaxies: active – galaxies: nuclei – galaxies: jets – quasars: emission lines – quasars: general

[1]Shanghai Astronomical Observatory, Chinese Academy of Sciences, Shanghai 200030, China
E-mail: yliu@center.shao.ac.cn

[2]National Astronomical Observatories, Chinese Academy of Sciences, Beijing 100012, China

[3]Graduate School of the Chinese Academy of Sciences, BeiJing 100039, China

1. INTRODUCTION

Relativistic jets observed in radio loud AGNs as an extreme phenomenon, congregated most attention in the past decades. The properties of relativistic radio jets are thought to be closely connected with the properties of both accretion disk and black hole in active galactic nuclei. However, the origin and formation of relativistic jets are still the unsolved mystery lying in astrophysics. The currently most favored models of the formation of the jet are Blandford-Znajek and Blandford-Payne mechanisms (Blandford & Znajek 1977; Blandford & Payne 1982). In both mechanisms, the accretion generated the power and extracted from the disk or black hole rotational energy and converted into the kinetic power of the jet. Moreover, the accretion process upon the central supermassive black hole is believed to be responsible for the activity of AGNs. It is thus conceivable that the radio activity is connected with the central black hole.

Since the correlation of black hole mass with radio luminosity was first suggested for a handful of galaxies (Franceschini, Vercellone & Fabian 1998), the issue of a possible dependence of radio activity on black hole mass has recently been the subject of many scientific debates (McLure et al. 1999; Lacy et al. 2001; Jarvis & McLure 2002; McLure & Jarvis 2004). Several studies claimed that the radio luminosity is tightly connected with the black hole mass (e.g. Laor 2000; Lacy et al. 2001; McLure et al. 2004) in the different samples. Recently, using a sample of about 6000 quasars from the SDSS, McLure & Jarvis (2004) proposed that both the radio luminosity and radio loudness are strongly correlated with the black hole mass, although the range in radio luminosity at a given black hole mass is several orders of magnitude. However, several authors have claimed that no strong link exists between the black hole mass and radio luminosity in AGNs (e.g. Oshlack, Webster & Whiting 2002; Woo & Urry 2002a; Ho 2002; Urry 2003; Snellen et al. 2003). Woo & Urry (2002a) showed that the black hole mass ranges are not different between radio loud and radio quiet samples with 377 AGNs, and the strong correlation between black hole mass and radio luminosity is not found. Moreover, Oshlack et al. (2002) found no indication of correlation between the radio luminosity and black hole mass for a sample of radio-selected, flat-spectrum quasars (see Jarvis & McLure 2002 for a different interpretation).

In spite of these widely contrasting results, it is worth noting that the radio emission is commonly used in the above mentioned works, however, this can be problematic for radio loud AGNs. Due to the significant Doppler enhancement in the relativistic jets, the total radio luminosity is only a poor indicator of intrinsic jet power. Specifically, the majority of core-dominated blazar-like quasars have incredibly strong 5 GHz flux density from emission on the subkiloparsec scale, yet they have weak or moderate radio lobe emission (Punsly 1995). Moreover, the radio emission dissipated in the jet only represents the part of the jet

power, and most of the energy in the jets is not radiated away but is transported to the lobes. Thus, the radio emission is an indirect measurement of the energy transported through the jets from the central engine. Physically, a far better way is to investigate the relationship between the jet power and black hole mass. Usually, the jet power as a fundamental radio parameter to indicate the energy transported through the radio jet from the central engine, can not be readily obtained. Nevertheless, it can be estimated from studying the isotropic properties of the material ejected from the ends of the jets in the radio lobes. Rawlings & Saunders (1991) estimated $Q_{\rm jet}$, the bulk kinetic power as a token of total starting jet kinetic power, under the main assumption that the electrons and the magnetic field make an equal contribution to the total energy density. Then from a total lobe energy E, an efficiency η that allows for work done on the external medium, and a lobe age T, the $Q_{\rm jet}$ can be derived by using $Q = E/T\eta$. Recently, Willott et al. (1999) presented a sophisticated calculation of the jet power utilizing the optically thin flux density from the lobes measured at 151 MHz, which incorporates the deviations from the minimum-energy estimates in a multiplicative factor f that represents the small departures from minimum energy, geometric effects, filling factors, protonic contributions, and the low-frequency cutoff.

More recently, motivated by recent X-ray observations, Punsly (2005) presented a theoretical derivation of an estimate for a radio source jet power, by assuming that most of the energy in the lobes is in plasma thermal energy with a negligible contribution from magnetic energy (not equipartition), and computing the elapsed time from spectral ageing. The basic idea is that lobe expansion is dictated by the internal dynamics of the lobes and the physical state of the enveloping extragalactic gas. The expression yields jet powers that are quantitatively similar (to within a factor of 2) to the more sophisticated empirical relation of Willott et al. (1999) and Blundell & Rawlings (2000), in spite of the fact that U, the energy stored in the lobes, and T, the elapsed time, are determined from completely different methods and assumptions. The formula allows one to estimate the jet power using the measurement of the optically thin radio lobe emission in quasars and radio galaxies. The close agreement of the two independent expressions makes them robust estimators of jet power.

Usually, the radio loudness can be used to indicate the radio properties, and to distinguish radio quiet and radio loud populations. It is conventionally defined as $R \equiv L_{\nu 5{\rm GHz}}/L_{\nu 4400}$, and the boundary between the two populations was set at R = 10 (Visnovsky et al. 1992; Stocke et al. 1992; Kellermann et al. 1994). In the radio loud objects, R generally locates in the range 10 - 1000, and most radio quiet objects fall in the range 0.1 - 1 (Peterson 1997). An alternative criterion to distinguish the radio loud and radio quiet objects is based on the radio luminosity alone, which set a limitation at $P_{\rm 6cm} \approx 10^{25}$ W Hz^{-1} sr^{-1} (Miller, Peacock & Mead 1990). According to these criterion, just only $10\% - 20\%$ was qualified as radio loud objects in optical selected samples (e.g. Kellermann et al. 1989; Hooper et al. 1995).

However, some studies questioned this distribution by using radio selected samples (e.g. Wadadekar & Kembhavi 1999; White et al. 2000). Ho & Peng (2001) recalculated the radio loudness with the measurement of nuclear component for a sample of Syfert 1 galaxies, and claimed that at least 60% of sources in their sample are characterized by $R \geq 10$, and then territory traditionally reserved for radio loud AGNs. Similarly, the radio loudness calculation can also be questioned, due to the fact that the observed luminosity at 5 GHz of radio loud AGNs has been extremely Doppler boosted, and the intrinsic luminosity can be (much) lower. The Doppler enhancement of relativistic flows in jets is a crucial parameter since the total luminosity of an unresolved jet scales as the Doppler factor to the fourth power and to the third power for a resolved cylindrical jet (Lind & Blandford 1985). Moreover, the Doppler enhancement of the synchrotron emission of the jet may also hold at optical bands, thus the optical emission may be dominated by the beamed non-thermal synchrotron emission for radio loud AGNs in general, Flat Spectrum Radio Quasars (FSRQs) in particular. Consequently, this effect must be considered when the radio loudness is used to indicate the radio properties for radio loud AGNs, although the accurate correction for individual object is rather difficult.

The primary goal of this paper is to investigate the issue of whether the jet power and black hole mass are related in the radio loud AGNs, by calculating the jet power and black hole mass. We also try to define a new radio loudness by eliminating the Doppler boosting effects. Then, we explore the connection between the radio loudness and black hole mass. § 2 presents the sample and § 3 depicts the methods to estimate jet power, black hole mass, broad line region luminosity, and new-defined radio loudness. The results and discussions are shown in § 4. In last section, § 5, we will give the conclusions. Throughout the paper, we adopt the spectral index convention $f_\nu \propto \nu^{-\alpha}$ and a cosmology with $H_0 = 70$ km s^{-1} Mpc^{-1}, $\Omega_M = 0.3$, $\Omega_\Lambda = 0.7$. All values of luminosity used in this paper are corrected to our adopted cosmological parameters.

2. Sample Selection

We started this work with the quasars and BL Lac objects in the 1 Jy, S4 and S5 radio source catalogues (all sources identified as galaxies have not been considered here) which has the VLA extended radio 5 GHz observations. To estimate the black hole mass and broad line region luminosity, we then searched the literature for available measurements of the full width at half maximum (FWHM) of one of broad Hβ, MgII, CIV lines, as well as the line flux of these lines. Finally, the sample of 146 radio loud quasars is constructed, of which 79 are FSRQs with $\alpha_{2\mathrm{GHz}-8\mathrm{GHz}} < 0.5$ and 67 are Steep Spectrum Radio Quasars (SSRQs) with

$\alpha_{2\mathrm{GHz}-8\mathrm{GHz}} > 0.5$.

Table 1 gives the list of our sample with the relevant information for each object. Columns (1) - (3) represent the object's IAU name, redshift, and radio spectrum type labeled from the spectral index between 2 GHz and 8 GHz (FS is for flat spectrum and SS denotes steep spectrum), respectively. In Columns (4) and (5), we list the jet power derived from the extended radio flux density and the references for radio extended flux density, respectively. Columns (6) - (8) list the broad line region luminosity, the adopted broad line and its corresponding references, respectively. In Columns (9) - (11), we present the black hole mass, the adopted line for FWHM and its references, respectively. The conventional and new-defined radio loudness are listed in Columns (12) and (13), respectively (see details in § 3.3). A more detailed notation is given at the end of Table 1.

The extended radio luminosity has been K-corrected to 5 GHz in the source rest frame, assuming $\alpha = 1.0$. Fig. 1 shows the redshift distribution along with the radio total luminosity at 5 GHz (Fig. 1a) and radio extended luminosity at 5 GHz (Fig. 1b). It can be seen that almost all sources locate in the redshift range $0.1 < z < 2.5$, and both the total and extended 5 GHz radio luminosities cover about four orders of magnitude. When FSRQs and SSRQs are nearly indistinguishable in total 5 GHz luminosity, the extended luminosities of FSRQs are statistically lower than those of SSRQs.

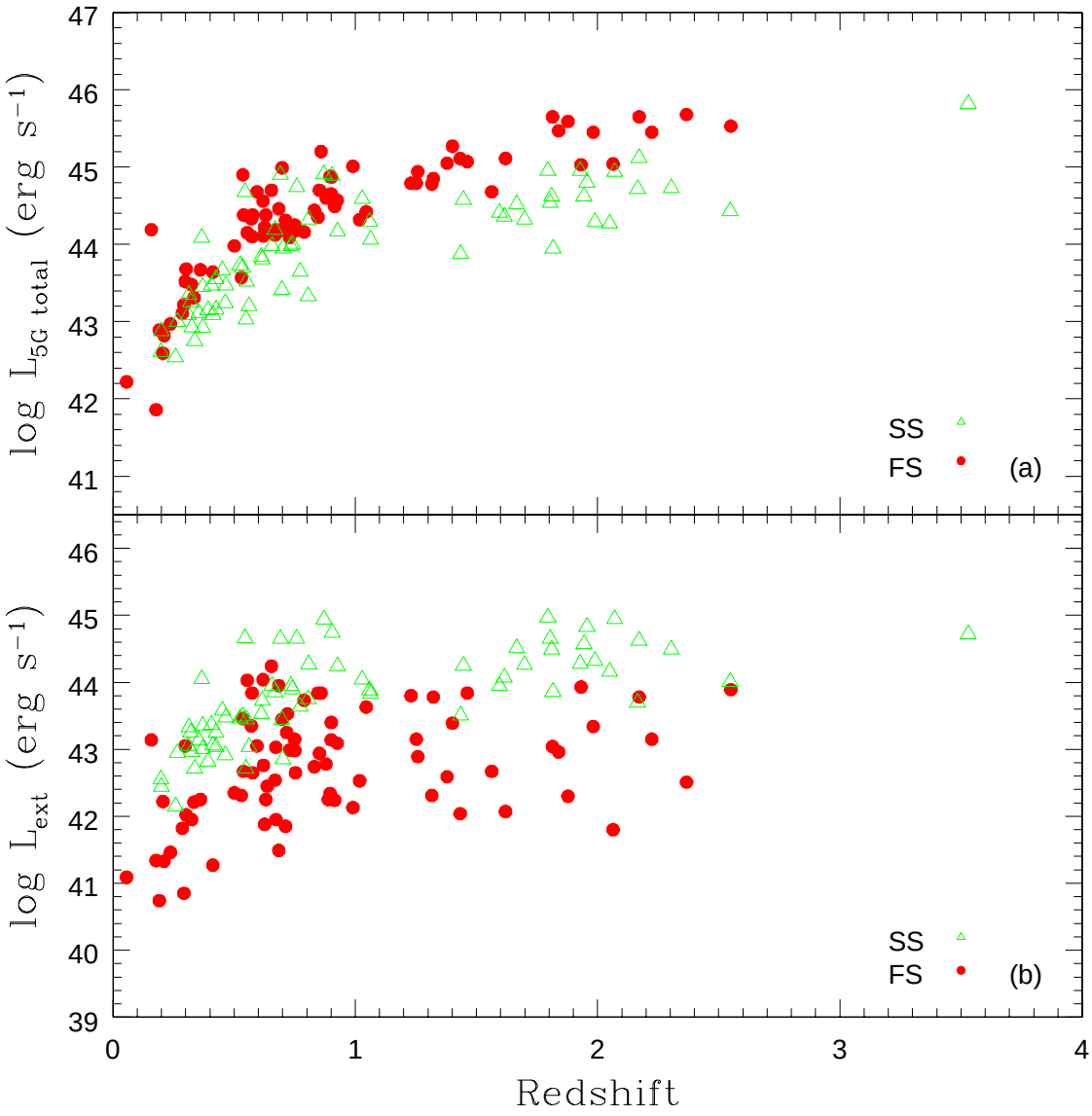

Fig. 1.— (a) The total 5 GHz radio luminosity versus redshift; (b) The radio extended luminosity at 5 GHz versus redshift. The solid circles display FSRQs ($\alpha < 0.5$), and the open triangles show SSRQs ($\alpha > 0.5$). The spectral index α is derived from 8 GHz to 2 GHz.

Table 1. The Sample

Object	z	type	log Q_{jet}	Refs.	log L_{BLR}	Line	Refs.	log M_{BH}	Line	Refs.	log R	log R_*
0017+154	2.070	SS	47.19	BM87	45.79	C IV	C91	9.62	Mg II	H02	3.34	3.35
0022−297	0.406	SS	45.61	K98	44.15	Hβ	S93	7.81	Hβ	G01	4.40	4.30
0056−001	0.717	FS	45.49	BM87	44.91	Hβ	B96	8.37	Hβ	B96	3.58	2.85
0101−025	2.050	SS	46.40	R99	45.69	Mg II	C91	8.47	Mg II	C91	3.00	2.90
0119+041	0.637	FS	44.69	BM87	44.63	Hβ	JB91	8.65	Hβ	G01	4.34	2.62
0119−046	1.928	SS	46.52	R99	46.00	Mg II	SS91	9.91	Mg II	B94b	2.92	2.25
0122−042	0.561	SS	45.28	R99	44.16	Mg II	W86	8.61	Mg II	W86	2.53	2.37
0133+207	0.425	SS	45.50	BM87	45.02	Hβ	JB91	9.45	Hβ	H02	3.56	3.26
0134+329	0.367	SS	46.30	BM87	44.96	Hβ	JB91	8.65	Hβ	C97	3.53	3.49
0135−247	0.831	FS	44.98	BM87	45.36	Hβ	JB91	9.11	Hβ	G01	3.34	1.87
0159−117	0.669	FS	44.79	WB86	45.34	Hβ	O84	9.26	Hβ	B96	3.03	1.90
0212+735	2.367	FS	44.75	NH90	44.95	Mg II	L96	6.96	Mg II	L96	4.50	1.81
0226−038	2.064	FS	44.03	B00	45.90	C IV	O94	8.92	Hβ	M99	2.96	0.60
0237−233	2.224	FS	45.38	BM87	46.79	Hβ	B94a	9.57	Hβ	G01	3.18	0.97
0238+100	1.816	SS	46.10	N89	45.59	C IV	C91	9.48	C IV	C91	2.14	2.06
0248+430	1.316	FS	44.55	CJ01	45.27	Mg II	S93	8.49	Mg II	B94b	3.25	1.61
0333+321	1.258	FS	45.13	BM87	45.93	Mg II	SS91	9.25	Mg II	B94b	2.37	1.41
0336−019	0.852	FS	45.18	BM87	45.00	Hβ	JB91	8.89	Hβ	G01	4.06	2.48
0349−146	0.616	SS	45.97	WB86	45.67	Hβ	M96	9.97	Hβ	M96	2.64	2.56
0352+123	1.616	SS	46.30	N89	45.45	Mg II	C91	8.49	Mg II	C91	3.20	2.90
0403−132	0.571	FS	45.60	BM87	45.25	Hβ	O84	9.08	Hβ	M96	3.67	3.02
0405−123	0.574	FS	46.08	BM87	45.91	Hβ	O84	9.35	Hβ	M96	2.47	2.51
0406−127	1.563	FS	44.91	N89	44.96	C IV	W86	9.21	C IV	W86	3.51	2.32
0413−210	0.808	SS	46.51	K98	43.99	Mg II	W86	8.18	Mg II	W86	3.85	3.80
0414−060	0.773	SS	45.88	BM87	45.72	C IV	O94	9.95	Hβ	B96	2.32	2.31
0420−014	0.915	FS	44.48	BM87	44.92	Mg II	B89	8.41	Hβ	B96	3.43	1.88
0424−131	2.165	SS	45.94	BM87	46.11	C IV	O94	9.76	Hβ	M99	2.88	1.86
0454−220	0.534	SS	45.73	WB86	45.84	Hβ	M96	9.57	Hβ	M96	2.71	2.49
0518+165	0.759	SS	46.89	BM87	45.04	Hβ	JB91	8.60	Hβ	G01	4.04	3.95
0537−441	0.896	FS	44.58	BM87	45.05	Mg II	W86	8.33	Mg II	W86	3.10	1.85
0538+498	0.545	SS	46.90	BM87	44.54	Hβ	L96	9.23	Hβ	G01	3.97	3.94
0602−319	0.452	SS	45.82	U81	44.49	Hβ	R84	9.02	Hβ	G01	3.74	3.64
0607−157	0.324	FS	44.20	BM87	43.56	Hβ	H78	7.32	Hβ	G01	3.00	3.37
0637−752	0.654	FS	46.48	CJ01	45.44	Hβ	T93	8.81	Hβ	G01	3.26	2.86
0711+356	1.620	FS	44.31	M93	45.80	Mg II	L96	8.14	Mg II	L96	3.08	1.02
0723+679	0.846	FS	46.08	U81	44.80	Hβ	L96	8.46	Hβ	G01	3.63	3.69
0736+017	0.191	FS	42.99	BM87	44.18	Hβ	JB91	7.86	Hβ	B96	2.95	1.21
0738+313	0.631	FS	44.50	BM87	45.78	Hβ	JB91	9.57	Hβ	B96	3.20	1.50
0740+380	1.063	SS	46.06	BM87	45.71	C IV	W95	9.09	Hβ	H03	2.92	2.68
0748+126	0.889	FS	44.48	M93	44.95	Mg II	W86	8.15	Mg II	W86	3.80	1.86
0802+103	1.956	SS	47.06	A94	46.24	C IV	C91	8.98	C IV	C91	3.49	3.52
0804+499	1.433	FS	44.28	M93	45.39	Mg II	L96	9.39	Mg II	L96	3.60	1.38
0809+483	0.871	SS	47.18	BM87	44.84	Hβ	L96	8.95	Hβ	L96	4.06	4.09
0836+710	2.172	FS	46.01	M93	46.43	Mg II	L96	9.36	Hβ	M99	3.34	2.46
0837−120	0.198	SS	44.79	R99	45.00	Hβ	B96	8.86	Hβ	B96	2.48	2.41
0838+133	0.684	FS	46.19	BM87	45.14	Hβ	JB91	8.67	Hβ	B96	3.64	3.57

Table 1—Continued

Object	z	type	log Q_{jet}	Refs.	log L_{BLR}	Line	Refs.	log M_{BH}	Line	Refs.	log R	log R_*
0850+581	1.322	FS	46.02	CJ01	45.66	Mg II	L96	8.49	Mg II	L96	3.63	2.69
0859+470	1.462	FS	46.08	M93	45.27	Mg II	L96	7.67	Mg II	L96	4.07	3.14
0903+169	0.412	SS	45.30	BM87	44.69	Hβ	B96	8.39	Hβ	B96	3.25	3.21
0906+015	1.018	FS	44.77	BM87	45.11	Mg II	B89	8.55	Mg II	W86	3.34	1.99
0906+430	0.668	SS	46.09	BM87	43.34	Hβ	L96	6.85	Hβ	G01	3.95	3.61
0923+392	0.698	FS	45.69	BM87	45.79	Hβ	L96	9.09	Hβ	L96	4.48	2.72
0945+408	1.252	FS	45.39	M93	45.59	Mg II	L96	8.60	Mg II	L96	3.50	2.10
0953+254	0.712	FS	44.09	BM87	44.97	Hβ	JB91	8.70	Hβ	G01	3.56	1.43
0954+556	0.901	FS	45.64	M93	44.98	Hβ	L96	7.87	Hβ	G01	3.81	3.62
0955+326	0.530	FS	44.55	WB86	45.35	Hβ	M96	9.29	Hβ	M96	2.51	1.69
1007+417	0.612	SS	45.77	WB86	45.71	Hβ	JB91	9.03	Hβ	B96	2.79	2.48
1011−282	0.258	SS	44.39	K98	45.05	Hβ	C97	8.50	Hβ	B96	2.56	2.17
1023+067	1.699	SS	46.50	BM87	45.07	Mg II	C91	8.99	Mg II	C91	3.10	3.04
1028+313	0.178	FS	43.59	BM87	44.37	Hβ	B96	8.44	Hβ	B96	2.40	1.59
1040+123	1.029	SS	46.27	BM87	45.11	Mg II	N79	8.76	Mg II	H02	3.41	2.86
1100+772	0.312	SS	45.30	BM87	44.83	Hβ	JB91	9.19	Hβ	B96	2.51	2.47
1103−006	0.426	SS	45.28	R99	45.07	Hβ	B96	9.27	Hβ	B96	2.54	2.42
1111+408	0.734	SS	46.19	BM87	45.57	Hβ	JB91	9.84	Hβ	G01	3.45	3.42
1117−248	0.466	SS	45.72	K98	43.59	Mg II	W86	8.93	Mg II	W86	3.00	3.00
1136−135	0.554	FS	46.27	WB86	45.20	Hβ	O84	8.45	Hβ	O02	3.11	3.73
1137+660	0.656	SS	46.19	BM87	45.85	Hβ	JB91	9.31	Hβ	H02	2.91	2.88
1148−001	1.982	FS	45.57	CJ01	46.41	C IV	B89	8.90	Mg II	B94b	3.55	1.87
1150+497	0.334	FS	44.46	CJ01	44.39	Hβ	B96	8.45	Hβ	B96	3.23	2.39
1156+295	0.729	FS	45.23	M93	44.90	Hβ	B96	8.54	Hβ	B96	3.17	2.70
1202−262	0.789	FS	45.97	K98	44.07	Hβ	B99	8.59	Hβ	G01	4.04	4.26
1226+023	0.158	FS	45.38	BM87	45.59	Hβ	JB91	8.92	Hβ	C97	3.14	2.17
1226+105	2.304	SS	46.72	G91	46.39	C IV	C91	9.65	C IV	C91	3.17	2.92
1229−021	1.045	FS	45.87	CJ01	45.68	Mg II	B89	8.70	Mg II	W86	3.34	2.52
1232−249	0.355	SS	45.38	K98	43.53	Mg II	W86	8.91	Mg II	W86	2.95	2.97
1237−101	0.753	FS	44.89	BM87	44.97	Mg II	S93	8.95	Hβ	O02	3.59	2.24
1250+568	0.321	SS	45.50	BM87	44.57	Hβ	JB91	8.31	Hβ	B96	3.56	3.56
1253−055	0.536	FS	45.70	BM87	44.64	Hβ	M96	8.28	Hβ	G01	4.60	3.45
1258+404	1.666	SS	46.75	CJ01	45.79	Mg II	C91	8.22	Mg II	C91	3.71	3.70
1302−102	0.286	FS	44.07	CJ01	44.91	Hβ	M96	8.51	Hβ	O02	2.28	2.33
1317+520	1.060	SS	46.12	H83	45.80	Mg II	SS91	9.01	Mg II	B94b	2.97	2.56
1318+113	2.171	SS	46.86	G91	45.86	C IV	C91	9.32	C IV	C91	3.88	3.38
1327−214	0.524	SS	45.70	K98	45.76	Hβ	C97	9.28	Hβ	C97	2.79	2.53
1334−127	0.539	FS	44.91	CJ01	44.18	Mg II	S93	7.98	Mg II	W86	3.75	3.25
1354+195	0.720	FS	45.77	WB86	45.93	Hβ	B96	9.38	Hβ	B96	2.89	2.25
1355−416	0.313	SS	45.58	CJ01	45.26	Hβ	T93	9.65	Hβ	C97	2.73	2.72
1424−118	0.806	SS	45.99	R99	45.76	Mg II	S89	9.18	Mg II	W86	1.99	2.41
1434−076	0.697	SS	45.68	R99	44.48	Mg II	W86	8.84	Mg II	W86	2.65	2.68
1442+101	3.530	SS	46.95	BM87	45.93	C IV	C91	9.93	Hβ	H03	3.52	2.42
1458+718	0.905	SS	46.98	BM87	45.47	Hβ	L96	8.77	Hβ	L96	3.64	3.49
1502+106	1.839	FS	45.19	BM87	45.57	Mg II	W86	8.74	Mg II	W86	4.15	1.95
1510−089	0.361	FS	44.50	BM87	44.65	Hβ	B96	8.20	Hβ	B96	3.17	2.28

Table 1—Continued

Object	z	type	log Q_{jet}	Refs.	log L_{BLR}	Line	Refs.	log M_{BH}	Line	Refs.	log R	log R_*
1512+370	0.371	SS	45.25	WB86	44.46	Hβ	M96	8.77	Hβ	C97	2.10	2.19
1545+210	0.266	SS	45.20	BM87	44.86	C IV	O94	8.90	Hβ	C97	3.00	2.95
1546+027	0.412	FS	43.52	M93	44.68	Mg II	B89	8.47	Hβ	O02	3.55	1.16
1559+173	1.944	SS	46.81	S90	45.66	Mg II	C91	9.25	Mg II	C91	2.90	2.85
1606+289	1.989	SS	46.56	BM87	45.61	C IV	C91	9.37	C IV	C91	3.05	3.09
1611+343	1.401	FS	45.63	BM87	45.91	C IV	W95	9.60	Hβ	G01	3.85	2.10
1618+177	0.551	SS	45.69	BM87	46.13	Hβ	M96	9.65	Hβ	H02	2.66	2.59
1622+238	0.927	SS	46.48	BM87	45.34	Mg II	SS91	9.53	Hβ	B96	3.27	3.33
1624+416	2.550	FS	46.13	P95	43.97	C IV	L96	6.35	C IV	L96	5.11	4.26
1629+120	1.795	SS	47.21	S90	45.63	C IV	C91	9.65	C IV	C91	3.62	3.65
1633+382	1.814	FS	45.28	BM87	45.84	Mg II	L96	8.67	Mg II	L96	4.18	2.04
1637+574	0.750	FS	45.39	M93	45.57	Hβ	L96	9.22	Hβ	M96	3.31	2.38
1641+399	0.594	FS	45.30	BM87	45.47	Hβ	L96	9.27	Hβ	M96	3.57	2.38
1642+690	0.751	FS	45.22	M93	43.86	Hβ	L96	6.85	Hβ	L96	4.13	4.09
1655+077	0.621	FS	45.00	M93	43.62	Mg II	W86	7.28	Mg II	W86	4.60	3.70
1656+053	0.879	FS	45.02	M93	46.26	Hβ	B96	9.74	Hβ	B96	3.03	1.14
1704+608	0.371	SS	45.60	BM87	44.91	Hβ	M96	9.49	Hβ	C97	2.51	2.41
1721+343	0.206	FS	44.47	WB86	44.63	Hβ	B96	8.01	Hβ	B96	2.73	1.69
1725+044	0.293	FS	43.09	BM87	44.08	Hβ	R84	7.72	Hβ	O02	3.03	1.33
1739+522	1.379	FS	44.83	BM87	45.16	Mg II	L96	9.32	Mg II	L96	4.01	1.82
1803+784	0.684	FS	43.73	M93	44.56	Hβ	L96	7.92	Hβ	L96	3.55	1.54
1828+487	0.691	SS	46.89	BM87	45.25	Hβ	L96	9.85	Hβ	G01	3.85	3.61
1845+797	0.056	FS	43.36	WB86	42.97	Hβ	L96	7.75	Hβ	L96	2.66	2.74
1857+566	1.595	SS	46.19	N89	45.71	Mg II	C91	9.11	Mg II	C91	2.73	2.27
1928+738	0.302	FS	44.26	M93	45.18	Hβ	M96	8.35	Hβ	L96	3.27	1.50
1954+513	1.230	FS	46.04	K90	45.39	Mg II	L96	9.18	Mg II	L96	3.67	2.91
1954−388	0.626	FS	44.12	CJ01	44.20	Hβ	T93	7.99	Hβ	O02	3.38	2.25
2024−217	0.463	SS	45.15	K98	43.63	Mg II	W86	8.28	Mg II	W86	3.52	3.19
2044−168	1.932	FS	46.17	N89	46.20	C IV	O94	9.42	C IV	W86	3.14	2.51
2120+168	1.805	SS	46.88	BM87	45.57	C IV	O94	9.68	Mg II	H02	2.91	3.01
2121+053	1.878	FS	44.53	BM87	45.90	Mg II	SS91	8.78	Mg II	B94b	3.77	0.96
2128−123	0.501	FS	44.59	CJ01	45.42	Hβ	T93	9.02	Hβ	O02	2.77	1.61
2135−147	0.200	SS	44.69	BM87	44.71	Hβ	JB91	9.03	Hβ	M96	2.79	2.35
2141+175	0.211	FS	43.58	BM87	44.26	C IV	O94	7.95	Hβ	M96	2.57	2.09
2143−156	0.701	SS	45.09	BM87	44.95	Mg II	W86	7.68	Hβ	O02	3.04	1.95
2145+067	0.990	FS	44.37	M93	45.78	Mg II	N79	8.87	Mg II	B94b	3.44	0.87
2155−152	0.672	FS	45.27	CJ01	43.70	Hβ	S89	7.14	Hβ	G01	3.51	4.23
2201+315	0.298	FS	45.29	BM87	45.46	Hβ	JB91	8.94	Hβ	M96	2.73	2.40
2203−188	0.619	FS	46.28	CJ01	44.16	Mg II	S89	8.19	Mg II	W86	4.40	4.44
2208−137	0.392	SS	45.07	WB86	43.65	Mg II	W86	7.97	Mg II	W86	2.84	2.51
2216−038	0.901	FS	45.38	BM87	45.79	Mg II	B89	9.08	Hβ	G01	3.40	2.12
2247+140	0.237	FS	43.71	CJ01	43.83	Hβ	C97	7.91	Hβ	C97	3.12	2.22
2251+113	0.326	SS	45.21	BM87	44.90	C IV	O94	8.93	Hβ	M96	2.34	2.36
2251+158	0.859	FS	46.08	BM87	45.68	Hβ	JB91	8.83	Hβ	G01	3.58	2.60
2255−282	0.926	FS	45.33	K98	45.84	Hβ	B99	8.92	Hβ	G01	3.28	1.66
2302−279	1.435	SS	45.75	R99	44.41	C IV	W86	8.97	Mg II	W86	2.55	2.18

Table 1—Continued

Object	z	type	log Q_{jet}	Refs.	log L_{BLR}	Line	Refs.	log M_{BH}	Line	Refs.	log R	log R_*
2310−322	0.337	SS	44.95	R99	45.26	Hβ	C97	9.21	Hβ	C97	2.47	2.43
2311+469	0.741	SS	46.15	S01	44.94	Hβ	SK93	9.36	Hβ	G01	3.12	3.02
2314−116	0.549	SS	44.95	R99	43.78	Mg II	W86	8.90	Mg II	W86	2.59	2.26
2320−312	2.547	SS	46.24	R99	46.09	C IV	C91	9.47	C IV	C91	2.97	2.55
2335−181	1.446	SS	46.48	R99	44.61	C IV	W86	9.30	C IV	W86	3.05	2.71
2344+092	0.673	FS	44.19	BM87	45.50	Hβ	JB91	8.89	Hβ	B96	2.81	0.87
2345−167	0.576	FS	44.90	BM87	44.38	Hβ	JB91	8.47	Hβ	G01	3.90	2.85
2354+144	1.810	SS	46.73	H83	45.75	Hβ	C91	9.37	Hβ	C91	3.17	3.04

Notes: Column (1): IAU source name. Column (2): redshift. Column (3): spectrum type. Column (4): jet power Q_{jet} in units of erg s^{-1}. Column (5): references of radio extended flux density in calculating jet power. Column (6): broad line region luminosity in units of erg s^{-1}. Column (7): the adopted lines in calculating broad line region luminosity. Column (8): references for lines. Column (9): black hole mass in units of $M_\odot$. Column (10): lines for estimating black hole mass. Column (11): references for lines. Column (12): conventionally defined radio loudness. Column (13): new-defined radio loudness, i.e. ratio of the extended radio luminosity to the thermal optical luminosity estimated from the broad line luminosity.

References: A94: Akujor et al. (1994). B94a: Baker et al. (1994). B94b: Brotherton et al. (1994). B89: Baldwin et al. (1989). B96: Brotherton (1996). B99: Baker et al. (1999). B00: Barthel et al. (2000). BM87: Browne & Murphy (1987). C91: Corbin (1991). C97: Corbin (1997). CJ01: Cao & Jiang (2001). G91: Garrington et al. (1991). G01: Gu et al. (2001). H78: Hunstead et al. (1978). H83: Hintzen et al. (1983). H02: Hough et al. (2002). H03: Hirst et al. (2003). JB91: Jackson & Browne (1991). K90: Kollgaard et al. (1990). K98: Kapahi et al. (1998). L96: Lawrence et al. (1996). M93: Murphy et al. (1993). M96: Marziani et al. (1996). M99: McIntosh et al. (1999). N79: Neugebauer et al. (1979). N89: Neff et al. (1989). NH90: Neff & Hutchings (1990). O84: Oke et al. (1984). O94: Osmer et al. (1994). O02: Oshlack et al. (2002). P95: Punsly (1995). R84: Rudy (1984). R99: Reid et al. (1999). S89: Stickel et al. (1989). S90: Saikia et al. (1990). S93: Stickel et al. (1993). S01: Saikia et al. (2001). SK93: Stickel & Kuhr (1993). SS91: Steidel & Sargent (1991). T93: Tadhunter et al. (1993). U81: Ulvestad et al. (1981). W86: Wilkes (1986). W95: Wills et al. (1995). WB86: Wills & Browne (1986).

3. Method

3.1. Jet Power

In this work, we will use the formula derived from Punsly (2005):

$$Q_{\rm jet} = 5.7 \times 10^{44}(1+z)^{1+\alpha}Z^2F_{151} \ \ {\rm erg\ s^{-1}} \quad (1)$$

$$Z \approx 3.31 - 3.65 \times [(1+z)^4 - 0.203(1+z)^3 + 0.749(1+z)^2 + 0.444(1+z) + 0.205]^{-0.125} \quad (2)$$

to estimate the jet power, where F_{151} is the optically thin flux density from the lobes measured at 151 MHz in units of Janskys, and the value of $\alpha \approx 1$ is suggested by the observations (Kellermann, PaulinyToth & Williams 1969) as a good fiducial value (see Punsly 2005 for more details).

It should be noted that the equation (1) is only valid when the optically thin extended emission is measured. In the radio selected sample, the radio emission at low frequency, e.g. 151 MHz, is usually dominated in the steep spectrum quasars. That is to say, the spectrum at low frequency is steep, which usually emerges from the non-beamed optically thin lobes. In actuality, most of our objects indeed show a steep spectrum at low frequency. For these sources, roughly, the radio 151 MHz flux density could be directly used in equation (1). However, we also find the flat spectrum at low frequency in some objects. This implies that the radio emission at low frequency is mainly optically thick, then the Doppler boosting still holds even at low frequency in these objects, which precludes the possibility of directly using the measured flux density in equation (1).

The extended radio flux measured from the optically thin lobes is free from the Doppler boosting effects, since the lobe material is generally thought to be of low enough bulk velocity. To further explore the validity of directly using the measured radio low frequency flux density in equation (1), we investigate the relationship between the flux density at 151 MHz and the extended flux density at 5 GHz in Fig. 2. It is apparent that there is a tight relationship between them for the sources with steep spectrum at low frequency (denoted by open triangles and open circles), since both of them are from the non-beamed optically thin lobes. However, large scatter and deviation exist in the sources with flat spectrum at low frequency (shown as solid triangles and solid circles). This is not surprising since the extended 5 GHz emission is from radio lobes, whereas the 151 MHz emission is mainly from radio cores, which is extremely Doppler boosted. These results show that it is problematic to directly use the low frequency radio flux density in equation (1), although it might be valid for the sources with steep spectrum at low frequency. Due to this fact, we extrapolate the extended 5 GHz flux density to calculate the extended 151 MHz flux density, by assuming a spectral index of $\alpha = 1.0$, in present work. The jet power is then estimated by substituting

the extrapolated extended 151 MHz flux density, instead of the measured 151 MHz flux density, in equation (1). The estimated jet power is listed in Column (4) of Table 1, where the references of the extended flux density at 5 GHz are given in Column (5).

3.2. Black hole mass and Broad line luminosity

The black hole mass can be estimated on the assumption that the dominant mechanism responsible for the width of the broad emission line is the gravitational potential of the central supermassive black hole, and that the line widths reflect the Keplerian velocities of the line-emitting material in a virialized system (Wandel, Peterson & Malkan 1999; McLure & Dunlop 2001). The black hole mass is given by

$$M_{BH} = R_{BLR} V^2 G^{-1} \tag{3}$$

where G is the gravitational constant, V is the velocity of the gas of broad emission line region gravitationally bound to the central black hole, and R_{BLR} is the size of the broad line region (BLR). V can be obtained directly form FWHM of the broad emission lines ($V = f \times V_{FWHM}$), where f is the factor that depends on the geometry and kinematics of the broad line region (McLure & Dunlop 2002; Vestergaard 2002). In present work, we adopt an uniform value $f = \sqrt{3}/2$ assuming an isotropic distribution of the broad line region clouds (Wandel 1999; Kaspi et al. 2000; Vestergaard 2002).

Besides estimating V from FWHM of the broad emission line, we need to estimate R_{BLR}. The reverberation mapping technique is the most reliable method to calculate R_{BLR}. The basic concept of this method is using the time lag of the emission line light with respect to the continuum light to estimate the light crossing size of the BLR. However, this method can be only used for a limited number of objects (Kaspi et al. 2000; Onken & Peterson 2002), since it requires intensive monitoring of the broad lines and the continuum.

The alternative and extensively used method to estimate R_{BLR} is to use the empirical relationship found between R_{BLR} and the optical continuum luminosity, which is inferred from the R_{BLR} determined from reverberation mapping method (Kaspi et al. 2000). Kaspi et al. (2000) have calibrated an empirical relation between the BLR size and the monochromatic luminosity at 5100 Å. Recently, Kaspi et al. (2005) reinvestigated the relationship between the characteristic R_{BLR} and the optical continuum luminosities, making use of the best available determinations of R_{BLR} for a large number of AGNs from Peterson et al. (2004). Simply averaging the measurements obtained from the BCES and FITEXY methods for the relation between R_{BLR} and the optical luminosity at 5100 Å, using one data point per object

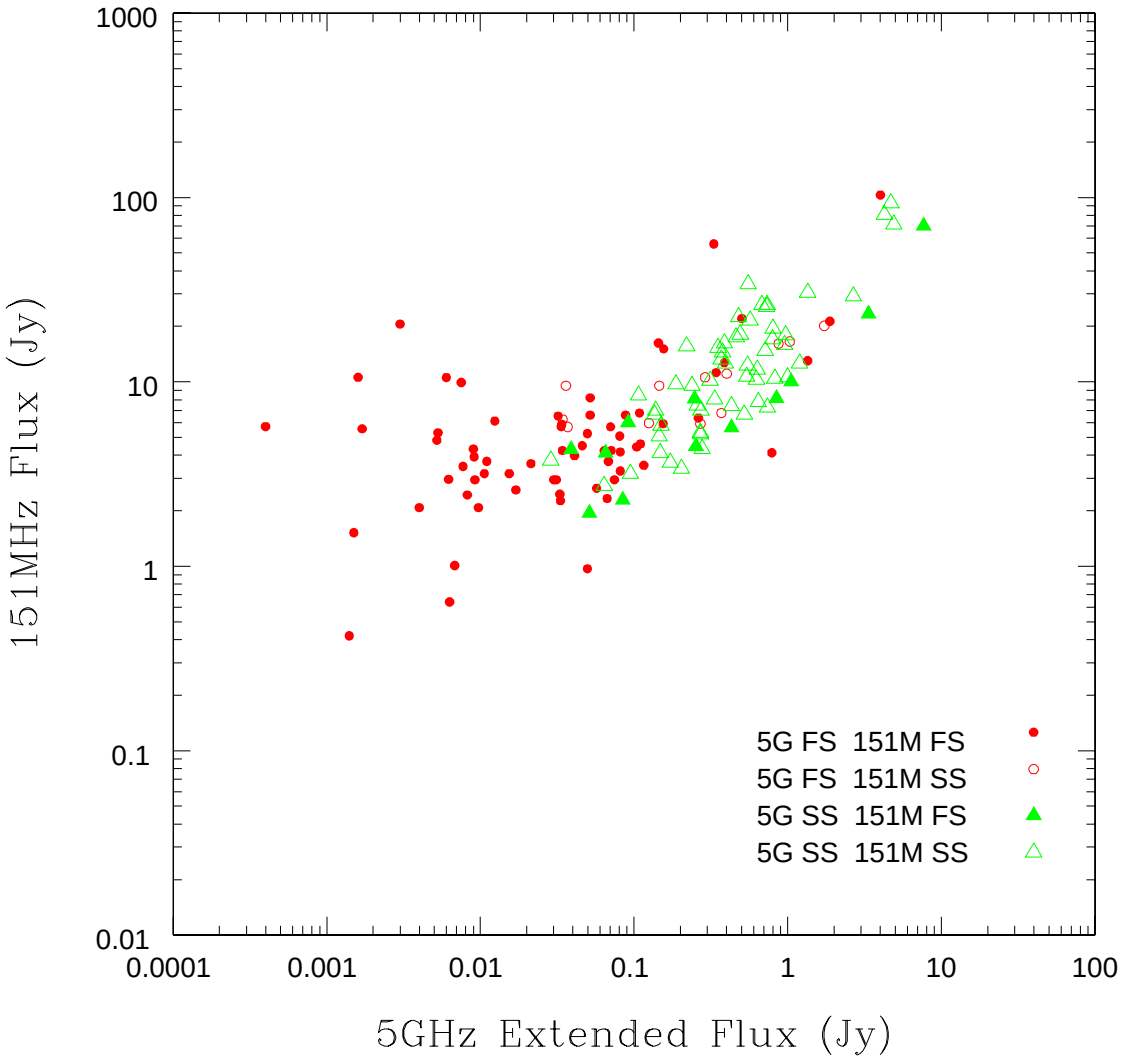

Fig. 2.— The relationship between the radio 5 GHz extended flux and the radio low frequency 151 MHz flux. The open triangles display the sources with steep spectrum both at high frequency (5 GHz) and low frequency (151 MHz); the solid triangles are the sources with steep spectrum at high frequency (5 GHz) but flat spectrum at low frequency (151 MHz); the open circles show those with flat spectrum at high frequency (5 GHz) but steep at low frequency (151 MHz); the solid circles denote those with flat spectrum both at high (5 GHz) and low frequency (151 MHz).

(see Kaspi et al. 2005), they found:

$$R_{BLR} = 22.30\ (\frac{\lambda L_{\lambda}(5100\text{Å})}{10^{44}\ \text{erg s}^{-1}})^{0.69}\ \ \text{lt} - \text{days} \tag{4}$$

Combining the R_{BLR} estimated from this formula and the FWHM of broad Hβ line measured from single-epoch spectrum, we can calculate the black hole mass using equation (3). However, Hβ line will be redshifted out of optical domain for the objects with relatively high redshift. Thus, this method is highly limited for high redshift objects (actually, Hβ line of six high redshift sources in our sample have been measured from IR spectrum, but usually IR spectrum is not readily available). McLure & Jarvis (2002) presented the expression to estimate black hole mass through calibrating the empirical relationship between the R_{BLR} and optical continuum luminosity for broad MgII.

$$\frac{M_{BH}}{M_{\odot}} = 3.37 \left(\frac{\lambda L_{3000}}{10^{44}\ \text{erg s}^{-1}}\right)^{0.47} \left(\frac{\text{FWHM(MgII)}}{\text{km s}^{-1}}\right)^{2} \tag{5}$$

This enables us to estimate black hole mass for high redshift AGNs, using the measured FWHM of broad MgII. Moreover, reverberation studies indicate that the size of the BLR for C IV is about half that of Hβ (Stirpe et al. 1994; Korista et al. 1995; Peterson 1997; Peterson & Wandel 1999). If we assume that $R_{BLR}(\text{CIV}) = 0.5R_{BLR}$, where R_{BLR} is derived from equation (4) (Corbett et al. 2003; Warner et al. 2003, 2004; Dietrich & Hamann 2004), then we can estimate the black hole mass with the FWHM of broad CIV.

Similar as the radio luminosity, the optical luminosity of radio loud quasars can also be contaminated by the effect of relativistic beaming. In fact, the optical emission of radio loud quasars is a mixture of thermal and non-thermal emission. In general, SSRQs tend to be orientated with jets pointing away from our line of sight, and FSRQs tend to be orientated with their jets beamed along our line of sight, although not explicitly applicable on a source-by-source basis. Thus, the optical emission may be dominated by the beamed non-thermal synchrotron emission in FSRQs. However, for SSRQs, even if the non-thermal synchrotron emission can extend to optical band, the steep spectrum and very weak beaming effect make it hardly possible to dominate over the thermal emission. Since the relationship between the BLR radius and optical continuum luminosity is supposed to be valid in the case of a thermal continuum, we thus must estimate the thermal optical continuum luminosities. In present work, we will calculate the thermal optical luminosity only for FSRQs. For SSRQs, we will use the optical luminosity directly as thermal optical luminosity, since the thermal optical emission dominates in these sources.

In the radio quiet AGNs, the optical emission is believed to be free from the contamination of non-thermal synchrotron emission since their jets are very weak (if present). The

broad emission line emission, which is produced by the illumination of ionizing luminosity from central AGNs on the BLR gas, can be used as a good indicator of the thermal optical emission. Therefore, we can estimate the thermal optical luminosity for FSRQs, by assuming that their thermal optical luminosities exhibit a dependence on broad emission line luminosities similar to that of radio quiet AGNs. We fitted the Hβ line (in erg s^{-1}) and optical luminosities (in erg s^{-1}) to a power-law using the Ordinary Least Square (OLS) bisector method on the sample of radio quiet AGNs of Kaspi et al. (2000), and obtained the dependence:

$$L_{5100\mathrm{A}^{\circ}} = 0.843 \times 10^2 \; L_{\mathrm{H}\beta}^{0.998} \tag{6}$$

The relation of broad Hβ line and optical continuum luminosity and the fitted line is shown in Fig. 3. For FSRQs with the optical continuum luminosity exceeding the power-law dependence of equation (6), we adopt the continuum luminosities computed with equation (6) at the corresponding broad Hβ line luminosity. When Hβ is not available, we firstly calibrate the MgII or CIV lines to Hβ line adopting the relative flux of the relevant lines of the composite spectrum of Francis et al. (1991), respectively, then use equation (6) to estimate the thermal optical luminosity when the optical continuum luminosity exceeds the power-law dependence of equation (6). Hereafter, we will call the thermal optical luminosity estimated in this way as the thermal corrected optical luminosity. The relationship between the thermal corrected optical luminosity and measured optical luminosity for FSRQs is shown in Fig. 4. Due to the significant beaming effect, the large deviations from the equivalent line is apparently seen. This strengthens the necessity of removing beaming effect in optical band for FSRQs.

After computing the thermal corrected optical continuum luminosity of FSRQs and the optical luminosity of SSRQs (uncorrected), we then estimate the black hole mass by using equation (4) and FWHM of broad Hβ for 92 objects. When only Mg II line is available, we use FWHM of broad MgII line in combination with equation (5). For the rest 11 sources, we estimate the BLR size of CIV assuming that $R_{\mathrm{BLR}}(\mathrm{CIV}) = 0.5R_{\mathrm{BLR}}$, then combine FWHM value in equation (3) to estimate the black hole mass. Although this assumption may bring uncertainties in black hole mass, the small number fraction ($\sim 7.5\%$) may not influence our results. The calculated black hole mass, the line adopted and the corresponding references are shown in Table 1.

Following Celotti et al. (1997), the BLR luminosity is derived by scaling several strong emission lines to the quasar template spectrum of Francis et al. (1991), in which Lyα is used

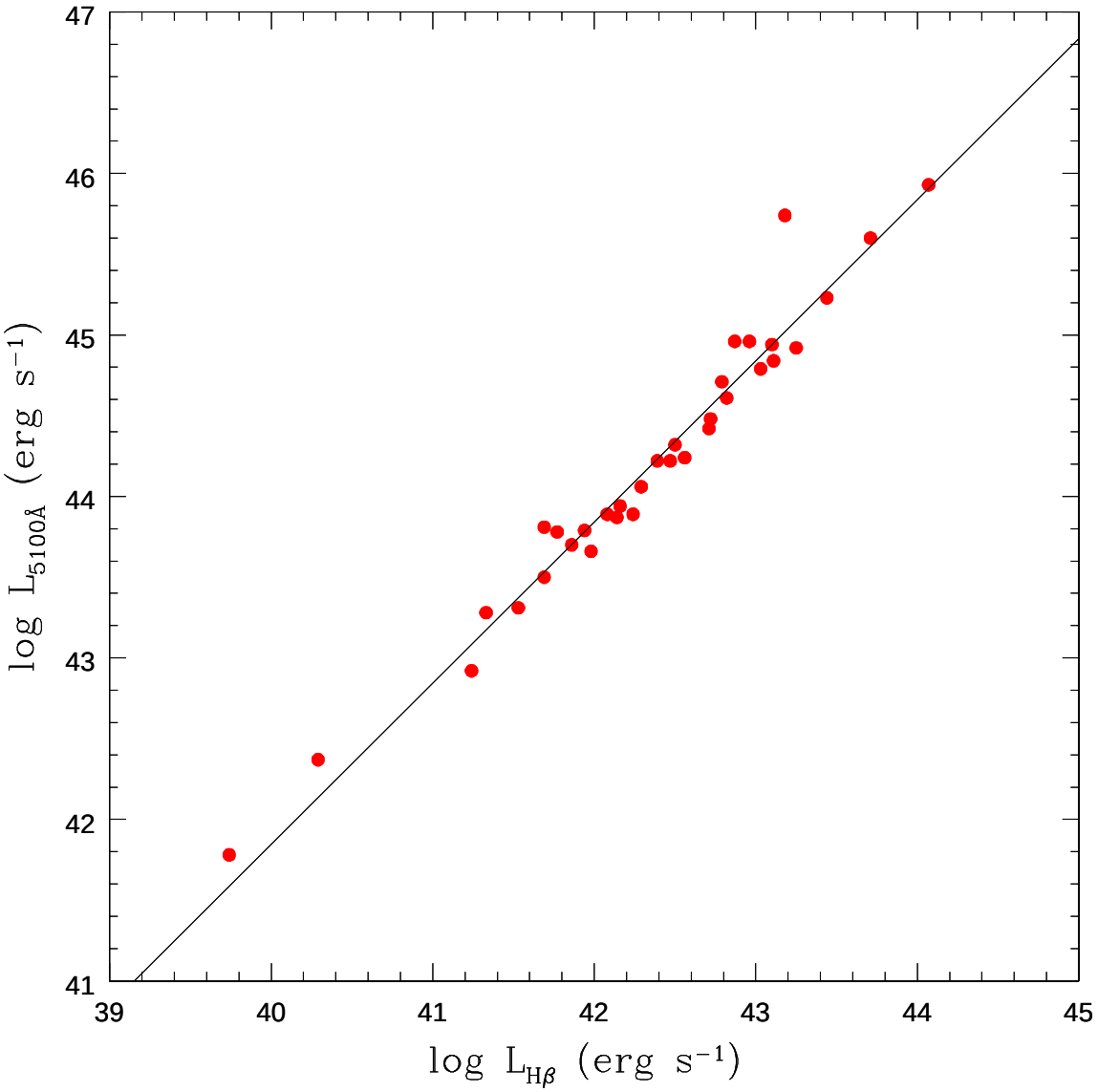

Fig. 3.— The broad Hβ line luminosity and the optical continuum luminosity at 5100 Å for a sample of radio quiet AGNs of Kaspi et al. (2000). The solid line is the fitted line using OLS method. Data are from Kaspi et al. (2000), and has been transferred to our adopted cosmology frame.

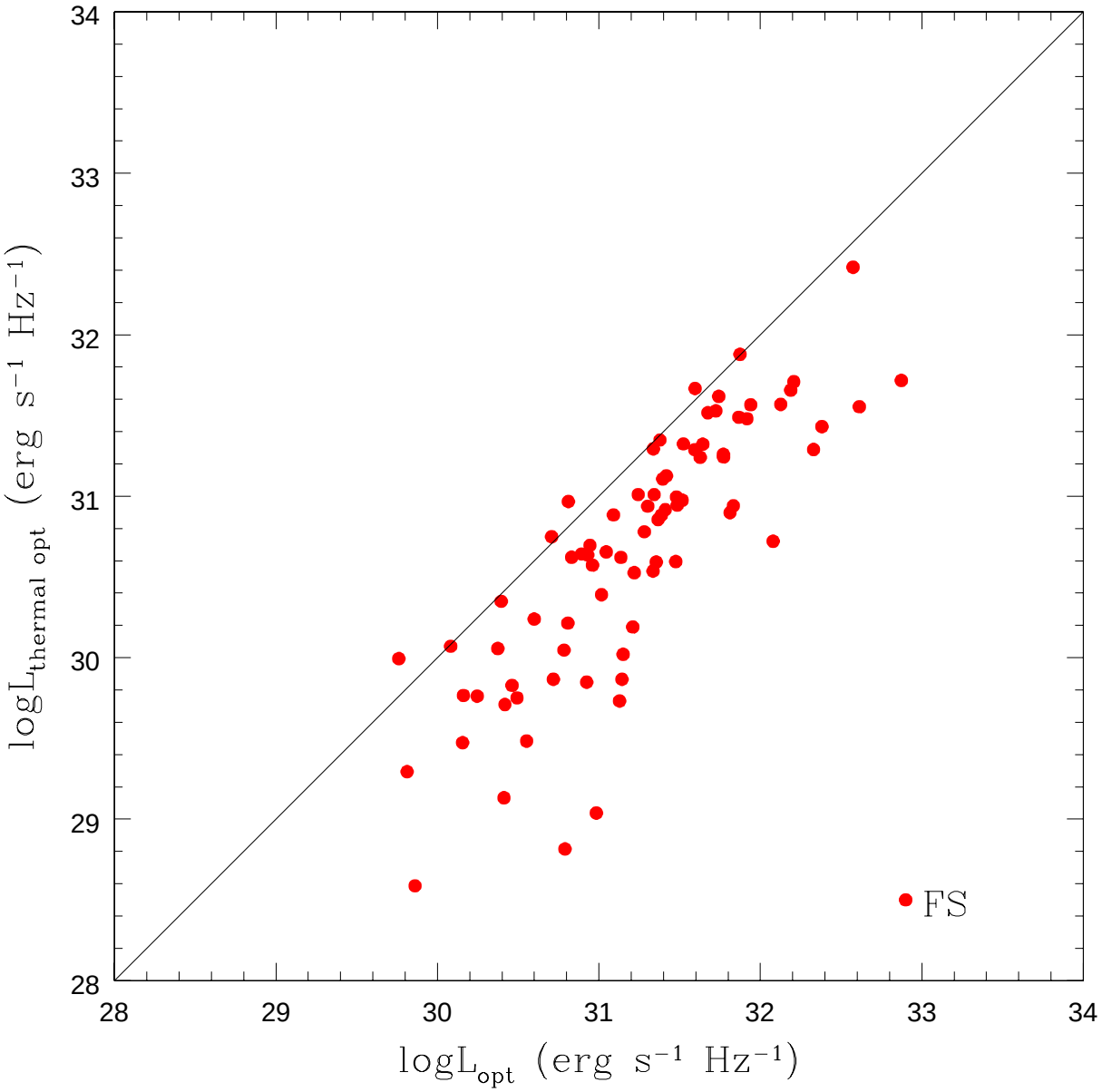

Fig. 4.— The thermal optical luminosity estimated using equation (6) and measured optical luminosity for FSRQs. The line is the equivalent line.

as a reference. From this approach,

$$L_{BLR} = \begin{cases} \frac{\langle L_{BLR} \rangle}{L_{est}(H\beta)} = 25.26 L_{H\beta}, \\ \\ \frac{\langle L_{BLR} \rangle}{L_{est}(MgII)} = 16.35 L_{Mg\ II}, \\ \\ \frac{\langle L_{BLR} \rangle}{L_{est}(CIV)} = 8.82 L_{C\ IV}, \end{cases} \quad (7)$$

where $\langle L_{BLR} \rangle = 555.77$, $L_{est}(H\beta) = 22$, $L_{est}(MgII) = 34$, and $L_{est}(CIV) = 63$. Table 1 gives the values of L_{BLR} estimated from Equation (7) in Column (6), as well as the adopted line in Column (7).

3.3. Radio loudness

The deficit of radio loudness in radio loud quasars lies in the effect of relativistic beaming both in radio and optical emission, especially for FSRQs. Actually, it has already been found that some radio loud quasars can be classified as radio quiet if the beaming effect of the jets are considered (so called 'radio intermediate quasars', see Falcke, Sherwood & Patnaik 1996; Jarvis & McLure 2002). To remove the beaming effect, it would be more reasonable to use the ratio of the intrinsic radio luminosity to thermal optical luminosity to estimate radio loudness, which can be a good indicator of the relative importance of radio emission.

In this work, we define a new radio loudness R_* as the ratio of the radio extended luminosity to the thermal corrected optical continuum luminosity to eliminate the effect of relativistic beaming. The conventional radio loudness R, and the new-defined radio loudness R_* are shown in Columns (12) and (13) of Table 1, respectively. These radio loudness are used to explore the relationship between them and the black hole mass, and the significance of beaming effect corrections in § 4.2.

4. Results and Discussions

4.1. Jet power, BLR luminosity and Black hole mass

The relationship between the jet power and black hole mass is shown in Fig. 5b. The triangles and circles represent the steep spectrum and flat spectrum quasars, respectively. We find a significant correlation between the Q_{jet} and M_{BH} with a correlation coefficient of $r = 0.419$ at $\gg 99.99$ per cent confidence. It should be noted with caution that this

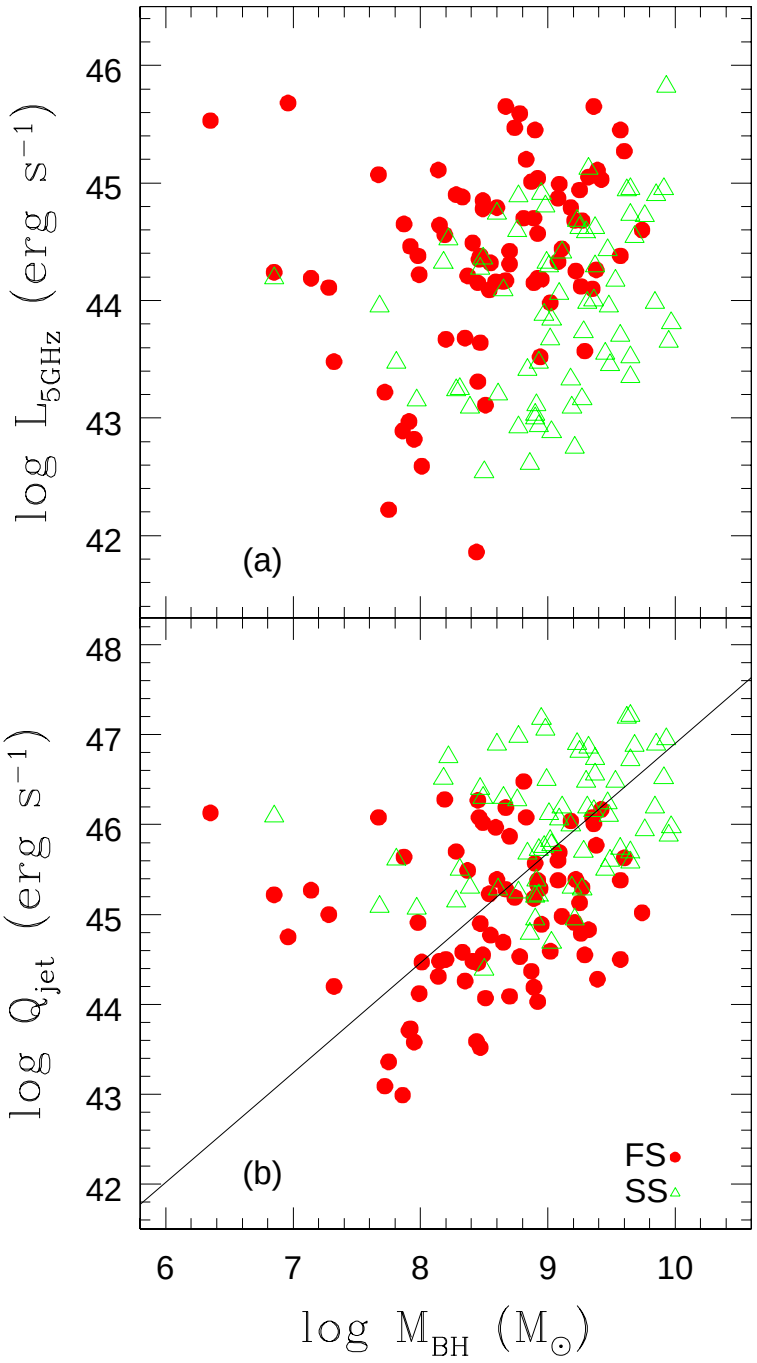

Fig. 5.— (a) The total radio 5 GHz luminosity vs. black hole mass. (b) The jet power vs. black hole mass. The solid circles denote FSRQs and the open triangles display SSRQs. The line is the fitted line using OLS method.

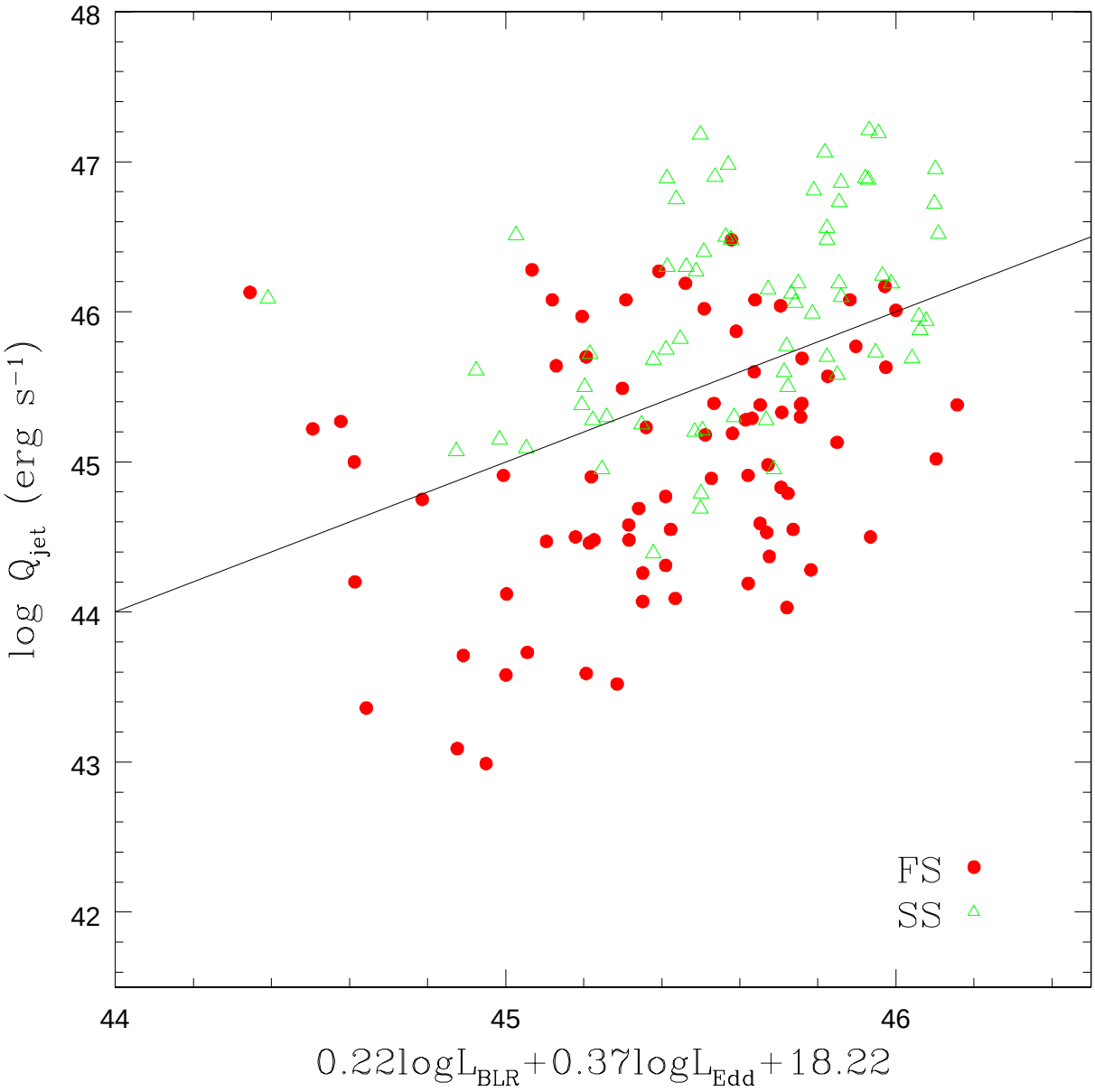

Fig. 6.— The relationship between the jet power and both the Eddington luminosity and the broad line region luminosity. The symbols are the same as in Fig. 5. The line is the least square multivariate regression line (equation (8)).

correlation may be caused by the common dependence of redshift. We therefore use the partial Spearman rank correlation method (Macklin 1982) to check this correlation. Still, the significant correlation with a correlation coefficient of 0.336 is present between Q_{jet} and M_{BH}, independent of the redshift. The significance of the partial rank correlation is 4.167, which is equivalent to the deviation from a unit variance normal distribution if there is no correlation present. So, the very strong correlation still holds while subtracting the common dependence of redshift. We conclude that this correlation is intrinsic for our sample of radio loud quasars. It therefore strongly supports the scenario of a tight connection between the relativistic jet and the black hole mass. The slope of the correlation of log Q_{jet} against log M_{BH} fitted using OLS method is 1.22 ± 0.09.

We also plot the relation of total 5 GHz radio luminosity against black hole mass in Fig. 5a. The Spearman rank correlation analysis shows a weak correlation with correlation coefficient r = 0.173 at 96.3 per cent confidence. Again, we use the partial Spearman rank correlation method to check this correlation by excluding the common dependence of redshift. However, we find no indication of correlation when subtracting the affecting of redshift. Thus, the apparent weak correlation might be a consequence of common dependence of redshift. In view of the significant intrinsic correlation between the jet power and black hole mass, it is likely that the different Doppler boosting in total radio luminosity, as well as the conversion rate of jet power to intrinsic radio luminosity from source to source, preclude the correlation to present between the total radio luminosity and black hole mass.

Motivated by the suggestion of the kinetic luminosity depending on both the disk luminosity and black hole mass (Wang, Luo & Ho 2004), we investigate the correlation between the jet power and both broad line region luminosity and black hole mass (in terms of its Eddington luminosity L_{Edd}). Using the least-squares method of multivariate regression, we find that Q_{jet} correlates with both L_{BLR} and L_{Edd} with correlation coefficient r = 0.432 and a probability of $p = 8.52 \times 10^{-8}$ for rejecting the null hypothesis of no correlation. The relationship can be expressed as:

$$\log Q_{jet} = (0.22 \pm 0.13) \log L_{BLR} + (0.37 \pm 0.14) \log L_{Edd} + (18.22 \pm 4.99) \quad (8)$$

This correlation (Fig. 6) suggests that the jet power depends on both the disk luminosity and black hole mass.

By defining the Eddington ratio as $\lambda = L_{bol}/L_{Edd}$, and assuming $L_{bol} \approx 10 L_{BLR}$, Equation (8) can be expressed in a different form as

$$\log Q_{jet} = 0.22 \log \lambda + 0.59 \log \left(\frac{M_{BH}}{M_{\odot}}\right) + 40.48 \quad (9)$$

This implies that the jet power depends on both the Eddington ratio and black hole mass, and

the black hole mass plays a dominant role in producing jet power, compared with Eddington ratio.

Despite the strong correlation exhibited in Fig. 6, clearly there is significant scatter. A significant fraction of this scatter may be due to measurement and/or systematic errors in Q_{jet}, L_{BLR}, and M_{BH}. When estimating the jet power, the extended 151 MHz flux density has been extrapolated from the VLA extended 5 GHz flux density, by adopting a spectral index $\alpha = 1.0$. An adoption of $\alpha = 0.7$ will bring a factor of about 3 uncertainty in the jet power. Moreover, it is likely that the part of low surface brightness radio emission could be undetectable in VLA radio images for some sources, which can also bring uncertainties in the jet power. Furthermore, the observed extended radio emission has been dissipated over a long period, thus, the jet power estimated from the past radio activity can be different from that of the time, at which the optical emission are observed. On the other hand, the uncertainty of black hole mass estimate using the line width-luminosity-mass relation is approximately a factor of 3 (Gebhardt et al. 2000; Ferrarese et al. 2001). However, it seems that all these uncertainties can not explain the large scatter in Fig. 6. Therefore, it is possible that the additional physical parameters, such as black hole spin or source environment, must also be included.

The beaming effect in radio luminosity has been noted by the Jarvis & McLure (2002) revisit of the radio luminosity - black hole mass relation after correcting Doppler boosting on the FSRQs sample of Oshlack et al. (2002). They found that the FSRQs occupy a wide range in intrinsic radio luminosity, and that many sources would be more accurately classified as radio-intermediate or radio-quiet quasars. Moreover, they claimed that FSRQs are fully consistent with an upper boundary on radio power of the form $L_{5GHz} \propto M_{BH}^{2.5}$. However, it should be noted that the Doppler boosting was only corrected averagely by adopting the average viewing angle of FSRQs (7°) and SSRQs (37°) (see Jarvis & McLure 2002 for more details). As the authors argued, both smaller and larger viewing angle are undoubtedly consistent with a Doppler boosting paradigm (and many of the sources will have $\theta < 7°$) for FSRQs. Recently, Woo et al. (2005) found that the radio luminosity and black hole mass are not correlated for a sample of BL Lac objects and FSRQs. Since an accurate beaming correction is not possible for individual object, the authors simply used the beam uncorrected radio luminosity. In spite of that, they argued that any beaming correction would unlikely reveal a hidden correlation between black hole mass and radio luminosity, given the fact that radio luminosity between FSRQs and BL Lac objects is different by a minimum of several orders of magnitude for the given black hole mass range. In this paper, we use the radio extended luminosity to indicate the intrinsic radio luminosity, since it is not affected by beaming effect. Even so, however, it can't be ignored that the radio luminosity is merely an indirect measure of the energy transported through the jets from the central

engine, and most of the energy in the jets is not radiated away but is transported to the lobes. Therefore, it's essential to explore the relationship between the fundamental radio parameter, namely, the jet power and the black hole mass. Our results in Fig. 5b show a very strong correlation between the black hole mass and the jet power for a sample of radio loud quasars. This intrinsic correlation indicates that the jet formation is closely connected with black hole mass.

By using the kinetic luminosity L_{Kin} calculated by Celotti et al. (1997), Wang et al. (2004) found L_{Kin} correlates with both L_{BLR} and M_{BH}. Moreover, they argued that the significant correlation between the kinetic luminosity and broad line region luminosity improved when the second parameter, M_{BH} is included. We have already shown that there is a significant correlation between the jet power and black hole mass, however, this correlation does not improve when including the broad line region luminosity. Notwithstanding this, interestingly, we find our results of equation (8) are consistent with that of Wang et al. (2004) within 1σ, in spite of the fact that we estimate the jet power on the sample of 146 radio loud quasars, whereas the kinetic luminosity is used in Wang et al. (2004) for a sample of only 35 blazars. The different fundamental radio parameters used on the different samples leading to the coherent results, suggests that the relationship between Q_{jet}, on both L_{BLR} and M_{BH} is likely fundamental in radio loud quasars, and the veracity of these two methods in calculating the power transported by the radio jets. Nevertheless, this relationship still need to be confirmed with a larger, and complete sample of radio loud quasars. In addition, it's more crucial to explore whether such relationship also holds for radio quiet AGNs, which might help us understand the difference between two populations.

4.2. Radio loudness and black hole mass

The comparison between R and R_* is shown in Fig. 7. It should be kept in mind that for new-defined radio loudness, using the radio extended luminosity to replace the total luminosity tends to decrease radio loudness, whereas using the thermal corrected optical luminosity tends to increase. Since corrections of optical luminosity in SSRQs are not committed presently, and their extended radio luminosity dominate in the total radio luminosity, SSRQs will be expected to stay tightly around $R_* = R$. This is apparently seen in Fig. 7. However, some sources stay somewhat away, but not much. This may be due to the variations of radio emission, or miss classification.

Conversely, the location of FSRQs in $R - R_*$ panel may vary from source to source, and depends on the amount of corrections in optical and radio luminosity since both of them are expected to be significant. This is obviously seen in Fig. 7, where a larger scatter

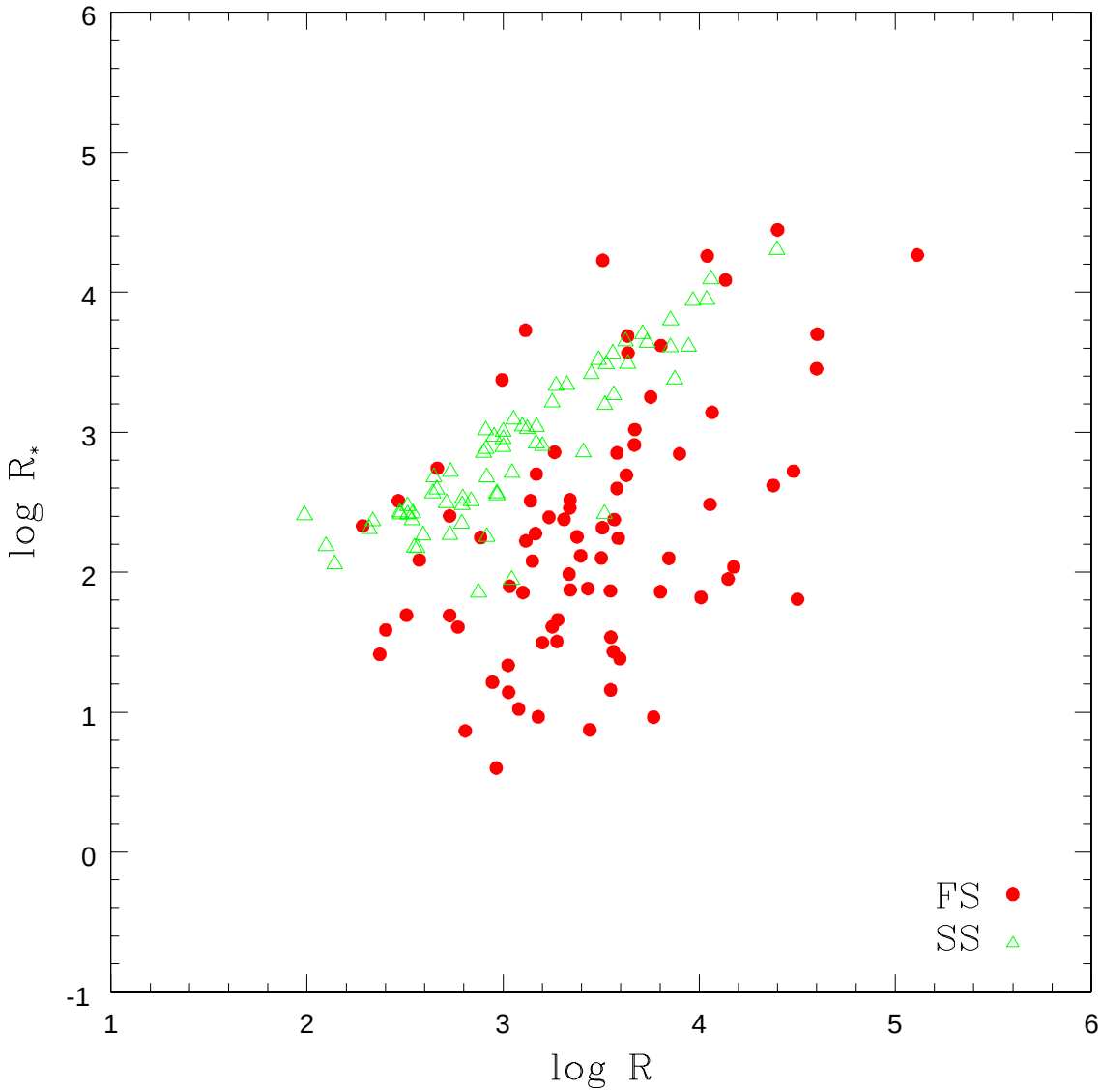

Fig. 7.— The relationship between R and R_*. R is the conventionally defined radio loudness, whereas R_* is the new-defined radio loudness as the ratio of radio extended luminosity to thermal optical continuum luminosity estimated from the broad line luminosity (see text). The symbols are the same as in Fig. 5.

presents for FSRQs. We find that for almost all FSRQs, R_* are smaller than R, which means that the beaming effect at radio band is dominated. The difference between R_* and R, i.e. the correction of R, cover a wide range of about three orders of magnitude. About half FSRQs have corrections ranging from 10 to 100, and about one fifth of FSRQs ranging in $100 - 1000$. In some extreme case, the correction is close to 1000. However, R_* can be greater than R in a few FSRQs. This implies that the optical luminosity in these sources are significantly dominated by the extremely Doppler boosted synchrotron emission resulting in the dominance of thermal correction. We note that for all FSRQs, the mean value of R is $< R >= 3.41$, whereas the mean value of R_* is $< R_* >= 2.25$ after correcting the effect of relativistic beaming in radio luminosity, as well as taking the thermal corrected optical luminosity. By adopting R_*, some of radio loud quasars should in fact be classified as radio intermediate and in some cases radio quiet.

We explore the relationship between the black hole mass and radio loudness R, and R_* in Fig. 8a, and Fig. 8b, respectively. Apparently, a significant anti-correlation between black hole mass and R presents in Fig. 8a. The Spearman rank correlation coefficient is found to be $r = -0.302$, with $\ll 0.01\%$ probability that no correlation is present. The detection of a significant anti-correlation between black hole mass and radio loudness is in good agreement with the Gu, Cao & Jiang (2001) study of a sample of radio loud quasars. However, Oshlack, Webster & Whiting (2002) attributed the apparent anti-correlation between the radio loudness and black hole mass to the consequence of using the optical flux in the measurement of black hole mass and also in the calculation of radio loudness, for a sample of FSRQs. Conversely, when the radio quiet AGNs are included, Lacy et al. (2001) found a strong correlation on the combined FBQS+PG sample. Moreover, Mclure & Jarvis (2004) found similar results using a sample of more than 6000 quasars from the SDSS, in which an upper limit in radio loudness was calculated for those quasars undetected by FIRST using the nominal FIRST object detection threshold of 1 mJy. In contrast, Woo & Urry (2002b) found no indication of an R - M_{BH} correlation in their study of a heterogeneous sample of 747 quasars in the redshift interval $1 < z < 2.5$ (although see McLure & Jarvis (2004) for a different interpretation).

However, we emphasize here that the conventional radio loudness R is severely contaminated by the effects of relativistic beaming in radio loud quasars as already shown in Fig. 7. Strictly, it may not be right to simply use R to indicate the radio property, with which further to investigate the relationship with other parameters, e.g. black hole mass in present. Whenever possible, the correction of beaming effect is required in calculating the fundamental (or intrinsic) radio loudness for FSRQs. Owing to the significance of corrections (as shown in Fig. 7), it's interesting to reinvestigate the correlation in Fig. 8a, by replacing with the new-defined radio loudness, and to see how the correction will influence

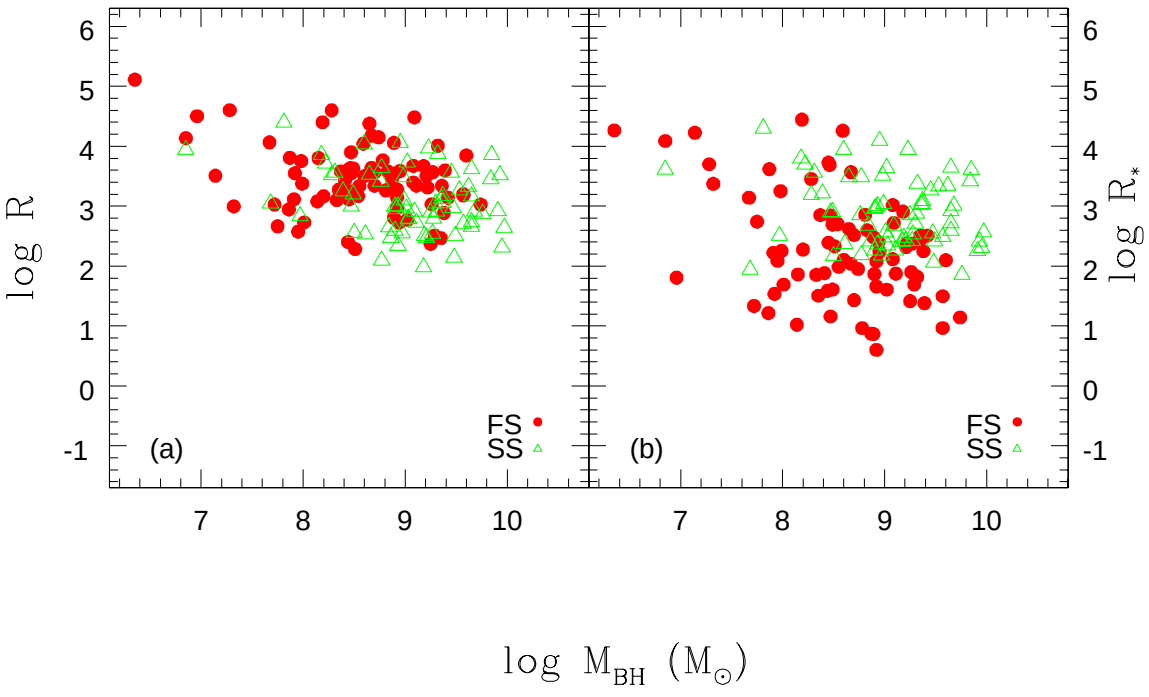

Fig. 8.— (a) The conventional radio loudness versus the black hole mass. (b) The new-defined radio loudness versus the black hole mass. The symbols are the same as in Fig. 5.

the correlation. Interestingly, the significant anti-correlation in Fig. 8a is not present in Fig. 8b. We then come to the conclusion that the black hole mass is not correlated with the new-defined radio loudness, although it was with the conventional radio loudness, at least for our sample of radio loud quasars. The significant anti-correlation in Fig. 8a might be predominately caused by beaming effect in radio luminosity and mistaking the beamed synchrotron emission dominated optical luminosity, if not all. These results further strengthen the importance of corrections in FSRQs, or radio loud quasars in general.

To further tackle the importance and necessity of corrections in radio loud quasars, we try to investigate the still debated issue of radio loudness dichotomy, by combining our radio loud quasars with a tentative sample of radio quiet quasars compiled from literature. The black hole mass of radio quiet quasars are estimated using the same methods as our radio loud quasars except that their optical luminosity is directly used. Their conventional radio loudness R are also calculated. The corrections in radio loudness are not considered since it's not important in radio quiet quasars. The distribution of conventional radio loudness R and new-defined radio loudness R_* is shown in the upper and lower panel of Fig. 9 for combined radio quiet and radio loud quasars, respectively. It can be seen from the upper panel that the gap around R=10, which is commonly used to distinguish radio quiet and radio loud AGNs, is apparently present. Although our combined sample is not complete, this is somehow consistent with the so-called radio-loudness dichotomy found in the optically selected quasars (Kellermann et al. 1989; Miller, Peacock & Mead 1990; Ivezić et al. 2002; also see Lacy et al. 2001 and Cirasuolo et al. 2003 for an alternative viewpoint). In the lower panel of Fig. 9, where the distribution of R of radio quiet quasars and new-defined radio loudness R_* of radio loud quasars are given, interestingly, we find that the radio loudness became continuously distributed, and the gap around 10 in the upper panel is not prominent. Expectedly, this result is simply the consequence of corrections in radio loud quasars, which makes enough radio loud quasars to fill in the gap. This result strengthens the significance of corrections. Moreover, it is likely suggestive that the uncorrections (both in radio and optical luminosity) in radio loud quasars may be partly (if not all) responsible for the observed radio loudness dichotomy in optically selected quasars. Notably, the incompleteness of our combined sample may preclude us to make solid conclusion. Nevertheless, the fact that the apparent gap in radio loudness distribution can be smoothed out after corrections, strongly demonstrates the necessity of correction.

The apparent non-prominence of a gap in new-defined radio loudness can also be clearly seen from the $R_* - M_{BH}$ relation in Fig. 10. Instead of no indication of correlation between the new-defined radio loudness and black hole mass in radio loud quasars alone (shown in Fig. 8b), we find a strong correlation in the combined sample. The Spearman rank correlation coefficient is found to be 0.451, at $\gg 99.99$ per cent confidence. This result is

in good agreement with that of McLure & Jarvis (2004) and Lacy et al. (2001). However, the scatter is large, and the range in radio loudness at a given black hole mass is several orders of magnitude. It's therefore clear that the influence of other physical effect, such as the accretion rate, black hole spin and source environment, must also be invoked to 'unify' the radio quiet and radio loud quasars.

5. Conclusions

By estimating the fundamental radio parameter, namely the jet power using the extended radio emission, we have investigated the relationship between the jet power and black hole mass for a sample of 146 radio loud quasars compiled from literature. Moreover, we define a new radio loudness as the ratio of radio extended luminosity to the thermal optical luminosity estimated from broad line luminosity. The relationship between the new-defined radio loudness and black hole mass was investigated. The main conclusions are summarized as follows:

- After removing the effect of relativistic beaming in the radio and optical emission, we find that the jet power is strongly correlated with black hole mass for radio loud AGNs. This correlation is proved to be intrinsic, and not an artefact of common dependence of redshift.

- When including the broad line region luminosity, we find that the jet power is correlated with both black hole mass and broad line region luminosity. The consistence with the Wang et al. (2004) study indicates that this correlation is likely fundamental in radio loud quasars. Moreover, we propose that the jet power correlates with both black hole mass and Eddington ratio.

- The correction in radio loudness is found to be significant in FSRQs. The strong anti-correlation between the conventional radio loudness and black hole mass is not present with new-defined radio loudness.

- Tentatively combining with a sample of radio quiet quasars, we find that the apparent gap in the conventional radio loudness is not prominent in the new-defined radio loudness. The necessity of correction on radio loudness is emphasized. The black hole mass is significantly correlated with the new-defined radio loudness in the combined sample.

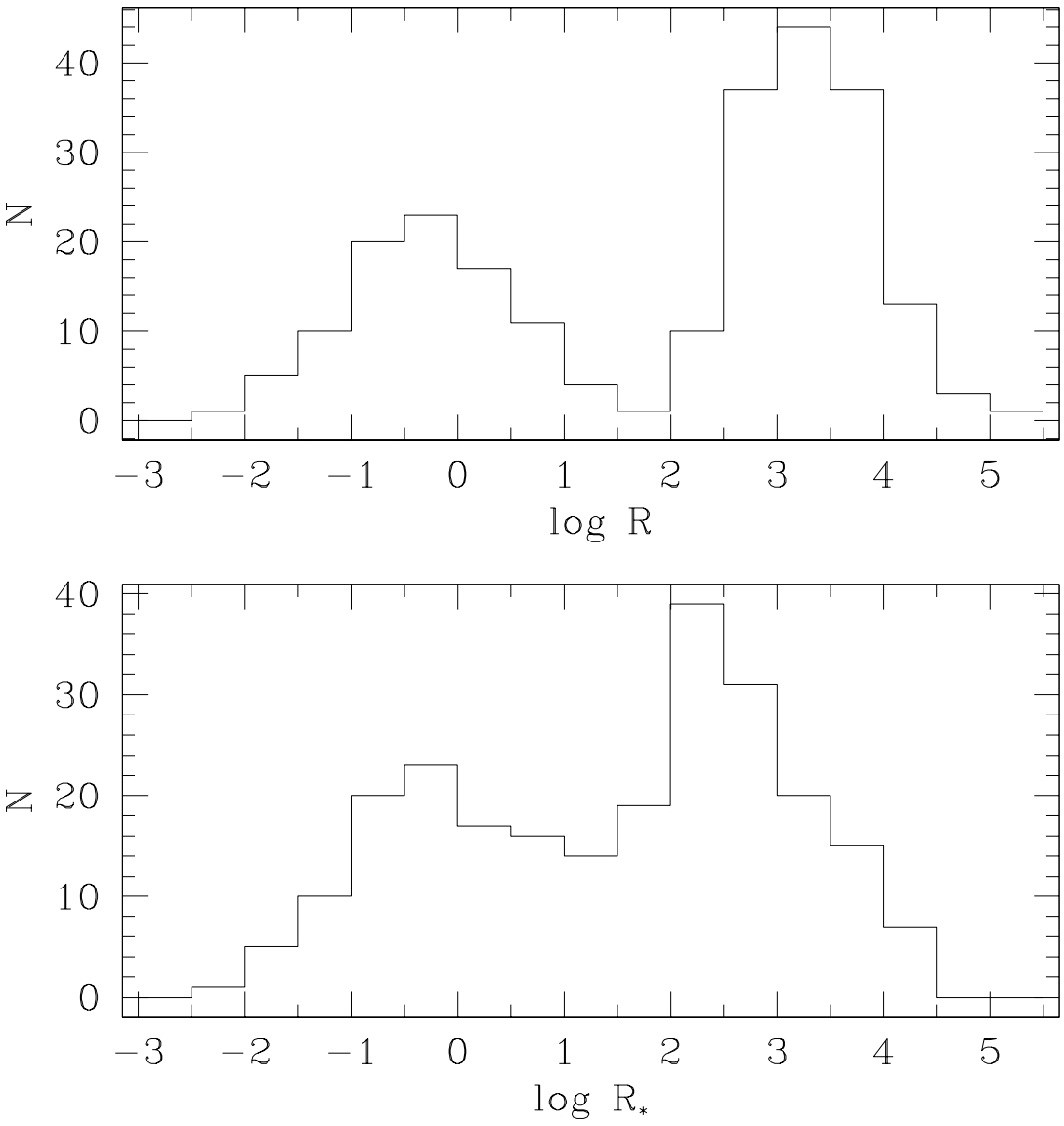

Fig. 9.— Distribution of the conventional radio loudness R (upper panel) and the new-defined radio loudness R_* (lower panel) for the combined sample of radio loud and radio quiet quasars.

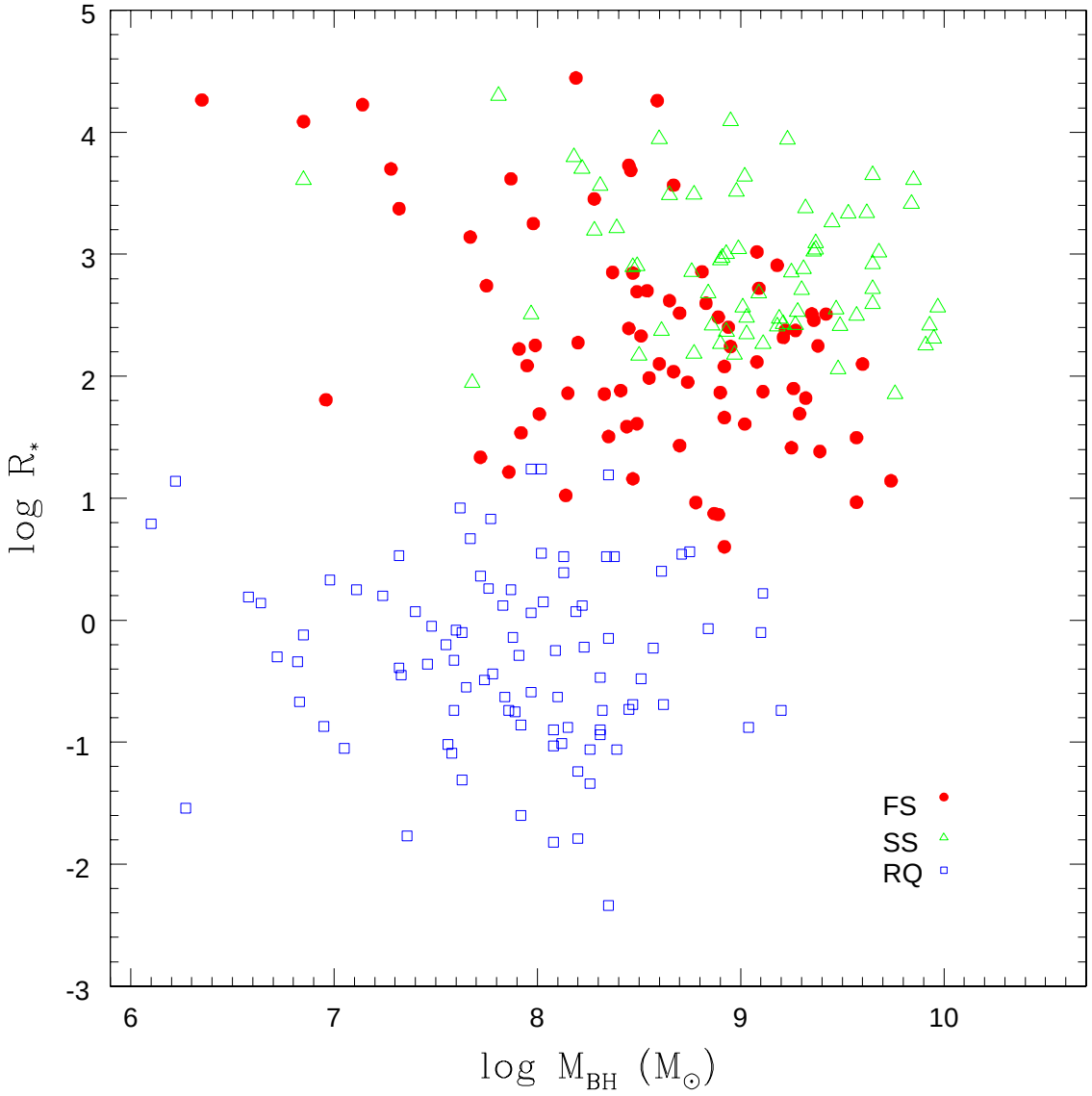

Fig. 10.— $R_* - M_{BH}$ relation for the combined sample of radio quiet and radio loud quasars. Solid circles are for FSRQs. Open triangles represent SSRQs, and open squares denote radio quiet quasars.

We are grateful to Xinwu Cao for helpful discussion. We thank the anonymous referee for insightful comments and constructive suggestions. This work is supported by NSFC under grants 10373019, 10333020 and G1999075403. This research has made use of the NASA/ IPAC Extragalactic Database (NED), which is operated by the Jet Propulsion Laboratory, California Institute of Technology, under contract with the National Aeronautics and Space Administration.

REFERENCES

Akujor, C. E., Luedke, E., Browne, I. W. A., Leahy, J. P., Garrington, S. T., Jackson, N. & Thomasson, P. 1994, A&AS, 105, 247 (A94)

Baker, A. C., Carswell, R. F., Bailey, J. A., Espey, B. R., Smith, M. G., & Ward, M. J. 1994, MNRAS 270, 575 (B94a)

Baker, J. C., Hunstead, R. W., Kapahi, V. K., & Subrahmanya, C. R. 1999, ApJS, 122, 29 (B99)

Baldwin, J. A., Wampler, E. J., & Gaskell, C. M. 1989, ApJ, 338, 630 (B89)

Barthel, P. D., Vestergaard, & Lonsdale, C. J. 2000, A &A, 354, 7 (B00)

Blandford, R. D., & Znajek, R. L. 1977, MNRAS, 179, 433

Blandford, R. D., & Payne, D. G. 1982, MNRAS, 199, 883

Blundell, K. M., & Rawlings, S. 2000, AJ, 119, 1111

Brotherton, M. S., Wills, B. J., Steidel, C. C., & Sargent, W. L. W. 1994, ApJ, 423, 131 (B94b)

Brotherton, M. S. 1996, ApJS, 102, 1 (B96)

Browne, I. W. A., & Murphy, D. W., 1987, MNRAS, 226, 601 (BM87)

Cao, X. W., & Jiang, D. R. 2001, MNRAS, 320, 347 (CJ01)

Celotti, A., Padovani, P., & Ghisellini, G. 1997, MNRAS, 286, 415

Cirasuolo, M., Celotti, A., Magliocchetti, M., Danese, L. 2003, MNRAS, 346, 477

Corbett, E. A., et al. 2003, MNRAS, 343, 705

Corbin, M. R. 1991, ApJ, 375, 503 (C91)

Corbin, M. R. 1997, ApJS, 113, 245 (C97)

Dietrich, M., & Hamann, F. 2004, ApJ, 611, 761

Falcke, H., Sherwood, W., & Patnaik, A. R. 1996, ApJ, 471, 106

Ferrarese, L., Pogge, R. W., Peterson, B. M., Merritt, D., Wandel, A., & Joseph, C. L. 2001, ApJ, 555, L79

Franceschini, A., Vercellone, S., & Fabian, A. C. 1998, MNRAS, 297, 817

Francis, P. J., Hewett, P. C., Foltz, C. B., Chaffee, F. H., Weymann, R. J., & Morris, S. L. 1991, ApJ, 373, 465

Garrington, S. T., Conway, R. G., & Leahy, J. P. 1991, MNRAS, 250, 171 (G91)

Gebhardt, K., et al. 2000, ApJ, 543, L5

Gu, M. F., Cao, X. W., & Jiang, D. R. 2001, MNRAS, 327, 1111 (G01)

Hintzen, P., Ulvestad, J., & Owen, F. 1983, AJ, 88, 709 (H83)

Hirst, P., Jackson, N., & Rawlings, S. 2003, MNRAS, 346, 1009 (H03)

Ho, L. C., & Peng, C. Y. 2001, ApJ, 555, 650

Ho, L. C. 2002, ApJ, 564, 120

Hooper, E. J., Impey, C. D., Foltz, C. B., & Hewett, P. C., 1995, ApJ, 445, 62

Hough, D. H., Vermeulen, R. C., Readhead, A. C. S., Cross, L. L., Barth, E. L., Yu, L. H., Beyer, P. J., & Phifer, E. M. 2002, AJ, 123, 1258 (H02)

Hunstead, R. W., Murdoch, H. S., & Shobbrook, R. R. 1978, MNRAS 185, 149 (H78)

Ivezić, Z., Menou, K., Knapp, G. R., Strauss, M. A., Lupton, R. H., Vanden, B. D. E., Richards, G. T., Tremonti, C., Weinstein, M. A., & Anderson, S. 2002, AJ, 124, 2364

Jackson, N., & Browne, I. W. A. 1991, MNRAS 250, 414 (JB91)

Jarvis, M. J. & McLure, R. J. 2002, MNRAS, 336, 38

Kapahi, V. K., Athreya, R. M., Subrahmanya, C. R., Baker, J. C., Hunstead, R. W., McCarthy, P. J., & Breugel, W. V. 1998, ApJS, 118, 327 (K98)

Kaspi, S., Smith, P. S., Netzer, H., Maoz, D., Jannuzi, B. T., & Giveon, U. 2000, ApJ, 533, 631

Kaspi, S., Maoz, D., Netzer, H., Peterson, B. M., Vestergarrd, M., & Jannuzi, B. T. (astro-ph/0504484)

Kellermann, K. I., Pauliny-Toth, I. I. K., & Williams, P. J. S. 1969, ApJ, 157, 1

Kellermann, K. I., Sramek, R., Schmidt, M., Shaffer, D. B., & Green, R. 1989, AJ, 98, 1195

Kellermann, K. I., Sramek, R. A., Schmidt, M., Green, R. F., & Shaffer, D. B. 1994, AJ, 108, 1163

Kollgaard, R. I., Wardle, J. F. C., & Roberts, D. H. 1990, AJ, 100, 1057 (K90)

Korista, K. T., et al. 1995, ApJS, 97, 285

Lacy, M., Laurent-Muehleisen, S. A., Ridgway, S. E., Becker, R. H., & White, R. L. 2001, ApJ, 551, L17

Laor, A. 2000, ApJ, 543, L111

Lawrence, C. R., Zucker, J. R., Readhead, A. C. S., Unwin, S. C., Pearson, T. J., & Xu, W. 1996, ApJS, 107, 541 (L96)

Lind, K. R., & Blandford, R. D. 1985, ApJ, 295, L358

Macklin, J. T. 1982, MNRAS, 199, 1119

Marziani, P., Sulentic, J. W., Dultzin-Hacyan, D., Calvani, M., & Moles, M. 1996, ApJS, 104, 37 (M96)

McIntosh, D. H., Rieke, M. J., Rix, H. W., Foltz, C. B., & Weymann, R. J. 1999, ApJ, 514, 40 (M99)

McLure, R. J., Kukula, M. J., Dunlop, J. S., Baum, S. A., O'Dea, C. P., & Hughes, D. H. 1999, MNRAS, 308, 377

McLure, R. J., & Dunlop, J. S. 2001, MNRAS, 327, 199

MuLure, R. J., & Dunlop, J. S. 2002, MNRAS, 331, 795

McLure, R. J., & Jarvis, M. J. 2002, MNRAS, 337, 109

McLure, R. J., Willott, C. J., Jarvis, M. J., Rawlings, S., Hill, G. J., Mitchell, E., Dunlop, J. S., & Wold, M. 2004, MNRAS, 351, 347

McLure, R. J., & Jarvis, M. J. 2004, MNRAS, 353, L45

Miller, L., Peacock, J. A., & Mead, A. R. G. 1990, MNRAS, 244, 207

Murphy, D. W., Browne, I. W. A., & Perley, R. A. 1993, MNRAS, 264, 298 (M93)

Neff, S. G., Hutchings, J. B., & Gower, A. C. 1989, AJ, 97, 1291 (N89)

Neff, S. G., & Hutchings, J. B. 1990, AJ, 100, 1441 (NH90)

Neugebauer, G., Oke, J. B., Becklin, E. E., & Matthews, K. 1979, ApJ, 230, 79 (N79)

Oke, J. B., Shields, G. A., & Korycansky, D. G. 1984, ApJ, 277, 64 (O84)

Onken, C. A., & Peterson, B. M. 2002, ApJ, 572, 746

Oshlack, A. Y. K. N., Webster, R. L., & Whiting, M. T. 2002, ApJ, 576, 81 (O02)

Osmer, P. S., Porter, A. C., & Green, R. F. 1994, ApJ, 436, 678 (O94)

Peterson, B. M. 1997, An Introduction to Active Galactic Nuclei (Cambridge: Cambridge Univ. Press)

Peterson, B. M., & Wandel, A. 1999, ApJ, 521, L95

Peterson, B. M., Ferrarese, L., Gilbert, K. M., Kaspi, S., Malkan, M. A., Maoz, D., Merritt, D., Netzer, H., Onken, C. A., Pogge, R. W., Vestergaard, M., &Wandel, A. 2004, ApJ, 613, 682

Punsly, B. 1995, AJ, 109, 1555 (P95)

Punsly, B. 2005, ApJ, 623, L9

Rawlings, S., & Saunders, R. 1991, Nature, 349, 10

Reid, R. I., Kronberg, P. P., & Perley, R. A. 1999, ApJS, 124, 285 (R99)

Rudy, R. J. 1984, ApJ, 284, 33 (R84)

Saikia, D. J., Junor, W., Cornwell, T. J., Muxlow, T. W. B., & Shastri, P. 1990, MNRAS, 245, 408 (S90)

Saikia, D. J., Jeyakumar, S., Salter, C. J., Thomasson, P., Spencer, R. E., & Mantovani, F. 2001, MNRAS, 321, 37 (S01)

Snellen, I. A. G., Lehnert, M. D., Bremer, M. N., & Schilizzi, R. T. 2003, MNRAS, 342, 889

Steidel, C. C., & Sargent, W. L. W. 1991, ApJ, 382, 433 (SS91)

Stickel, M., Fried, J. W., & Kühr H. 1989, A&AS, 80, 103 (S89)

Stickel, M., Kühr H., & Fried J. W. 1993, A&AS, 97, 483 (S93)

Stickel, M., & Kühr H. 1993, A&AS, 101, 521 (SK93)

Stirpe, G. M., et al. 1994, ApJ, 425, 609

Stocke, J. T., Morris, S. L., Weymann, R. J., & Foltz, C. B., 1992, ApJ, 396, 487

Tadhunter, C. N., Morganti, R., Alighieri, S. S., Fosbury, R. A. E., & Danziger, I. J. 1993, MNRAS, 263, 999 (T93)

Ulvestad, J., Johnston, K., Perley, R., & Fomalont, E. 1981, AJ, 86, 1010 (U81)

Urry, C. M. 2003, A&AS, 202, 2201

Vestergaard, M. 2002, ApJ, 571, 733

Visnovsky, K. L., Impey, C. D., Foltz, C. B., Hewett, P. C., Weymann, R. J., & Morris, S. L. 1992, ApJ, 391, 560

Wadadekar, Y., & Kembhavi, A. 1999, AJ, 118, 1435

Wandel, A., Peterson, B. M., & Malkan, M. A. 1999, ApJ, 526, 579

Wang, J. M., Luo, B., & Ho, L. C. 2004, ApJ, 615, L9

Warner, C., Hamann, F., & Dietrich, M. 2003, ApJ, 596, 72

Warner, C., Hamann, F., & Dietrich, M. 2004, ApJ, 608, 136

White, R. L., Becker, R. H., Gregg, M. D., Laurent-Muehleisen, S. A., & Brotherton, M. S., et. al. 2000, ApJS, 126, 133

Wilkes, B. J. 1986, MNRAS, 218, 331 (W86)

Willott, C. J., Rawlings, S, Blundell, K. M., & Lacy, M. 1999, MNRAS, 309, 1017

Wills, B. J., & Browne, I. W. A. 1986, ApJ, 302, 56 (WB86)

Wills, B. J., Thompson, K. L., Han, M., Netzer, H., Wills, D., Baldwin, J. A., Ferland, G. J., Browne, I. W. A., & Brotherton, M. S. 1995, ApJ, 447, 139 (W95)

Woo, J. H., & Urry, C. M. 2002a, ApJ, 579, 530

Woo, J. H., & Urry, C. M. 2002b, ApJ, 581, L5

Woo, J. H., Urry, C. M., Marel, R. P. van der, Lira, P., & Maza, J. (astro-ph/0506316)